Nambu-Goldstone modes and the Josephson supercurrent in the bilayer quantum Hall system

Yusuke Hama,[1,2] George Tsitsishvili,[3] and Zyun F. Ezawa[4]

[1]*Department of Physics, The University of Tokyo, Tokyo 113-0033, Japan*

[2]*Theoretical Research Division, Nishina Center, RIKEN, Wako 351-0198, Japan*

[3]*Department of Physics, Tbilisi State University, Tbilisi 0128, Georgia*

[4]*Advanced Meson Science Laborary, Nishina Center, RIKEN, Wako 351-0198, Japan*

(Dated: April 2, 2013)

Abstract

An interlayer phase coherence develops spontaneously in the bilayer quantum Hall system at the filling factor $\nu = 1$. On the other hand, the spin and pseudospin degrees of freedom are entangled coherently in the canted antiferromagnetic phase of the bilayer quantum Hall system at the filling factor $\nu = 2$. There emerges a complex Nambu-Goldstone mode with a linear dispersion in the zero tunneling-interaction limit for both cases. Then its phase field provokes a Josephson supercurrent in each layer, which is dissipationless as in a superconductor. We study what kind of phase coherence the Nambu-Goldstone mode develops in association with the Josephson supercurrent and its effect on the Hall resistance in the bilayer quantum Hall system at $\nu = 1, 2$, by employing the Grassmannian formalism.

I. INTRODUCTION

Quantum Hall (QH) effects are remarkable macroscopic quantum phenomena observed in the 2-dimensional electron system[1, 2]. They are so special in condensed matter physics that they are deeply connected with the fundamental principles of physics. Moreover, QH system provides us with an opportunity to enjoy the interplay between condensed matter physics and particle and nuclear physics[3].

In particular, the physics of the bilayer quantum Hall (QH) system is enormously rich owing to the intralayer and interlayer phase coherence controlled by the interplay between the spin and the layer (pseudospin) degrees of freedom[3, 4]. The interlayer phase coherence is an especially intriguing phenomenon in the bilayer QH system [3], where it is enhanced in the limit $\Delta_{\mathrm{SAS}} \to 0$. For instance, at the filling factor $\nu = 1$ there arises a unique phase, the spin-ferromagnet and pseudospin-ferromagnet phase, which has been well studied both theoretically and experimentally. One of the most intriguing phenomena is the Josephson tunneling between the two layers predicted in Refs.[5, 6], whose first experimental indication was obtained in Ref.[7]. Other examples are the anomalous behavior of the Hall resistance reported in counterflow experiments[8, 9] and in drag experiments[10]. They are triggered by the Josephson supercurrent within each layer[12]. Quite recently, careful experiments [11] were performed to explore the condition for the tunneling current to be dissipationless. These phenomena are produced by the pseudospins at $\nu = 1$, where the Nambu-Goldstone (NG) mode describes a pseudospin wave.

On the other hand, at $\nu = 2$ the bilayer QH system has three phases, the spin-ferromagnet and pseudospin-singlet phase (abridged as the spin phase), the spin-singlet and pseudospin fer-romagnet phase (abridged as the pseudospin phase) and a canted antiferromagnetic phase[14–17] (abridged as the CAF phase), depending on the relative strength between the Zeeman energy Δ_{Z} and the interlayer tunneling energy Δ_{SAS}. The pattern of the symmetry breaking is SU(4)→U(1)⊗SU(2)⊗SU(2), associated with which there appear four complex NG modes[18]. We have recently analyzed the full details of these NG modes in each phase[19]. The CAF phase is most interesting, where one of the NG modes becomes gapless and has a linear dispersion relation[19] as the tunneling interaction vanishes ($\Delta_{\mathrm{SAS}} \to 0$). It is an urgent and intriguing problem what kind of phase coherence this NG mode develops.

In this paper, we investigate the interlayer phase coherence, the associated NG modes, its effective Hamiltonian, the Josephson supercurrent provoked by these NG modes and its effect

to the Hall resistance in the bilayer QH system at $\nu = 1, 2$, by employing the Grassmannian formalism[18].

The basic field is the Grassmannian field consisting of complex projective (CP^3) fields. We introduce n CP^3 fields to analyze the $\nu = n$ bilayer QH system. The CP^3 field emerges when composite bosons undergo Bose-Einstein condensation[3]. We first make a perturbative analysis of the NG modes and reproduce the same results as obtained in [19]. We next analyze the nonperturbative phase coherent phenomena developed by the NG mode having linear dispersion, where the phase field $\vartheta(\mathbf{x})$ is essentially classical and may become very large, which is necessary to analyze the associated Josephson supercurrent. We show that it is the entangled spin-pseudospin phase coherence in the CAF phase. The Grassmannian formalism provides us with a clear physical picture of the spin-pseudospin phase coherence in the CAF phase, and, furthermore, enables us to describe nonperturbative phase-coherent phenomena uniformly in the bilayer QH system.

We then show that the Josephson supercurrent flows within the layer when there is inhomogeneity in $\vartheta(\mathbf{x})$. A related topic has been investigated in [20]. The supercurrent in the CAF phase leads to the same formula[12] for the anomalous Hall resistivity for the counterflow and drag geometries as the one at $\nu = 1$. What is remarkable is that the total current flowing in the CAF phase is a Josephson supercurrent carrying solely spins in the counterflow geometry. We also remark that the supercurrent flows both in the balanced and imbalanced systems at $\nu = 1$ but only in imbalanced systems at $\nu = 2$.

II. THE SU(4) EFFECTIVE HAMILTONIAN

Electrons in a plane perform cyclotron motion under perpendicular magnetic field $B_\perp$ and create Landau levels. The number of flux quanta passing through the system is $N_\Phi \equiv B_\perp S / \Phi_\mathrm{D}$, where S is the area of the system and $\Phi_\mathrm{D} = 2\pi\hbar/e$ is the flux quantum. There are N_Φ Landau sites per one Landau level, each of which is associated with one flux quantum and occupies an area $S/N_\Phi = 2\pi\ell_B^2$, with the magnetic length $\ell_B = \sqrt{\hbar/eB_\perp}$.

In the bilayer system an electron has two types of index, the spin index $(\uparrow, \downarrow)$ and the layer index (f, b). They can be incorporated in four types of isospin index, $\alpha = $ f$\uparrow$,f$\downarrow$,b$\uparrow$,b$\downarrow$. One Landau site may contain four electrons. The filling factor is $\nu = N/N_\Phi$ with N the total number of electrons.

We explore the physics of electrons confined to the lowest Landau level (LLL), where the electron position is specified solely by the guiding center $\boldsymbol{X} = (X, Y)$, whose X and Y components

3

are noncommutative,

$$[X, Y] = -i\ell_B^2. \tag{1}$$

The equations of motion follow from this noncommutative relation rather than the kinetic term for electrons confined within the LLL. In order to derive the effective Hamiltonian, it is convenient to represent the noncommutative relation with the use of the Fock states,

$$|n\rangle = \frac{1}{\sqrt{n!}}(b^\dagger)^n|0\rangle, \quad n = 0, 1, 2, \ldots, \quad b|0\rangle = 0, \tag{2}$$

where b and $b^\dagger$ are the ladder operators,

$$b = \frac{1}{\sqrt{2}\ell_B}(X - iY), \qquad b^\dagger = \frac{1}{\sqrt{2}\ell_B}(X + iY), \tag{3}$$

obeying $[b, b^\dagger] = 1$. Although the Fock states correspond to the Landau sites in the symmetric gauge, the resulting effective Hamiltonian is independent of the representation we have chosen.

We expand the electron field operator by a complete set of one-body wave functions $\varphi_n(\boldsymbol{x}) = \langle \boldsymbol{x}|n\rangle$ in the LLL,

$$\psi_\alpha(\boldsymbol{x}) \equiv \sum_{n=1}^{N_\Phi} c_\alpha(n)\varphi_n(\boldsymbol{x}), \tag{4}$$

where $c_\alpha(n)$ is the annihilation operator at the Landau site $|n\rangle$ with $\alpha = $ f↑,f↓,b↑,b↓. The operators $c_\alpha(m), c_\beta^\dagger(n)$ satisfy the standard anticommutation relations,

$$\{c_\alpha(m), c_\beta^\dagger(n)\} = \delta_{mn}\delta_{\alpha\beta}, \quad \{c_\alpha(m), c_\beta(n)\} = \{c_\alpha^\dagger(m), c_\beta^\dagger(n)\} = 0. \tag{5}$$

The electron field $\psi_\alpha(\boldsymbol{x})$ has four components, and the bilayer system possesses the underlying algebra SU(4), having the subalgebra $\text{SU}_{\text{spin}}(2) \times \text{SU}_{\text{ppin}}(2)$. We denote the three generators of the $\text{SU}_{\text{spin}}(2)$ by τ_a^{spin}, and those of $\text{SU}_{\text{ppin}}(2)$ by τ_a^{ppin}. There remain nine generators $\tau_a^{\text{spin}}\tau_b^{\text{ppin}}$, whose explicit form is given in Appendix A.

All the physical operators required for the description of the system are constructed as bilinear combinations of $\psi(\boldsymbol{x})$ and $\psi^\dagger(\boldsymbol{x})$. They are 16 density operators

$$\rho(\boldsymbol{x}) = \psi^\dagger(\boldsymbol{x})\psi(\boldsymbol{x}), \quad S_a(\boldsymbol{x}) = \frac{1}{2}\psi^\dagger(\boldsymbol{x})\tau_a^{\text{spin}}\psi(\boldsymbol{x}),$$

$$P_a(\boldsymbol{x}) = \frac{1}{2}\psi^\dagger(\boldsymbol{x})\tau_a^{\text{ppin}}\psi(\boldsymbol{x}), \quad R_{ab}(\boldsymbol{x}) = \frac{1}{2}\psi^\dagger(\boldsymbol{x})\tau_a^{\text{spin}}\tau_b^{\text{ppin}}\psi(\boldsymbol{x}), \tag{6}$$

where S_a describes the total spin and $2P_z$ measures the electron-density difference between the two layers. The operator R_{ab} transforms as a spin under $\text{SU}_{\text{spin}}(2)$ and as a pseudospin under $\text{SU}_{\text{ppin}}(2)$.

4

The kinetic Hamiltonian is quenched, since the kinetic energy is common to all states in the LLL. The Coulomb interaction is decomposed into the SU(4)-invariant and SU(4)-noninvariant terms

$$H_{\mathrm{C}}^+ = \frac{1}{2} \int d^2x d^2y V^+(\boldsymbol{x} - \boldsymbol{y}) \rho(\boldsymbol{x}) \rho(\boldsymbol{y}), \tag{7}$$

$$H_{\mathrm{C}}^- = 2 \int d^2x d^2y V^-(\boldsymbol{x} - \boldsymbol{y}) P_z(\boldsymbol{x}) P_z(\boldsymbol{y}), \tag{8}$$

where

$$V^\pm(\boldsymbol{x}) = \frac{e^2}{8\pi\epsilon} \left(\frac{1}{|\boldsymbol{x}|} \pm \frac{1}{\sqrt{|\boldsymbol{x}|^2 + d^2}} \right), \tag{9}$$

with layer separation d. The tunneling and bias terms are summarized into the pseudo-Zeeman term. Combining the Zeeman and pseudo-Zeeman terms we have

$$H_{\mathrm{ZpZ}} = - \int d^2x (\Delta_{\mathrm{Z}} S_z + \Delta_{\mathrm{SAS}} P_x + \Delta_{\mathrm{bias}} P_z), \tag{10}$$

with the Zeeman gap Δ_{Z}, the tunneling gap Δ_{SAS}, and the bias voltage $\Delta_{\mathrm{bias}} = eV_{\mathrm{bias}}$.

The total Hamiltonian is

$$H = H_{\mathrm{C}}^+ + H_{\mathrm{C}}^- + H_{\mathrm{ZpZ}}. \tag{11}$$

Note that the SU(4)-noninvariant terms vanish in the limit $d, \Delta_{\mathrm{Z}}, \Delta_{\mathrm{SAS}}, \Delta_{\mathrm{bias}} \to 0$.

We project the density operators (6) to the LLL by substituting the field operator (4) into them. A typical density operator reads

$$R_{ab}(\boldsymbol{p}) = e^{-\ell_B^2 \boldsymbol{p}^2/4} \hat{R}_{ab}(\boldsymbol{p}), \tag{12}$$

in momentum space, with

$$\hat{R}_{ab}(\boldsymbol{p}) = \frac{1}{4\pi} \sum_{mn} \langle n|e^{-i\boldsymbol{p}\boldsymbol{X}}|m\rangle c^\dagger(n) \tau_a^{\mathrm{spin}} \tau_b^{\mathrm{ppin}} c(m), \tag{13}$$

where $c(m)$ is the 4-component vector made of the operators $c_\alpha(m)$.

What are observed experimentally are the classical densities, which are expectation values such as $\hat{\rho}^{\mathrm{cl}}(\boldsymbol{p}) = \langle \mathfrak{S}|\hat{\rho}(\boldsymbol{p})|\mathfrak{S}\rangle$, where $|\mathfrak{S}\rangle$ represents a generic state in the LLL. The Coulomb Hamiltonian governing the classical densities are given by[21]:

$$
\begin{aligned}
H^{\mathrm{eff}} = {} & \pi \int d^2p V_D^+(\boldsymbol{p}) \hat{\rho}^{\mathrm{cl}}(-\boldsymbol{p}) \hat{\rho}^{\mathrm{cl}}(\boldsymbol{p}) + 4\pi \int d^2p V_D^-(\boldsymbol{p}) \hat{P}_z^{\mathrm{cl}}(-\boldsymbol{p}) \hat{P}_z^{\mathrm{cl}}(\boldsymbol{p}) \\
& - \frac{\pi}{2} \int d^2p V_X^d(\boldsymbol{p}) [\hat{S}_a^{\mathrm{cl}}(-\boldsymbol{p}) \hat{S}_a^{\mathrm{cl}}(\boldsymbol{p}) + \hat{P}_a^{\mathrm{cl}}(-\boldsymbol{p}) \hat{P}_a^{\mathrm{cl}}(\boldsymbol{p}) + \hat{R}_{ab}^{\mathrm{cl}}(-\boldsymbol{p}) \hat{R}_{ab}^{\mathrm{cl}}(\boldsymbol{p})] \\
& - \pi \int d^2p V_X^-(\boldsymbol{p}) [\hat{S}_a^{\mathrm{cl}}(-\boldsymbol{p}) \hat{S}_a^{\mathrm{cl}}(\boldsymbol{p}) + \hat{P}_z^{\mathrm{cl}}(-\boldsymbol{p}) \hat{P}_z^{\mathrm{cl}}(\boldsymbol{p}) + \hat{R}_{az}^{\mathrm{cl}}(-\boldsymbol{p}) \hat{R}_{az}^{\mathrm{cl}}(\boldsymbol{p})] \\
& - \frac{\pi}{8} \int d^2p V_X(\boldsymbol{p}) \hat{\rho}^{\mathrm{cl}}(-\boldsymbol{p}) \hat{\rho}^{\mathrm{cl}}(\boldsymbol{p}),
\end{aligned} \tag{14}
$$

5

where V_D and V_X are the direct and exchange Coulomb potentials, respectively,

$$V_D(\boldsymbol{p}) = \frac{e^2}{4\pi\epsilon|\boldsymbol{p}|}e^{-\ell_B^2\boldsymbol{p}^2/2}, \quad V_X(\boldsymbol{p}) = \frac{\sqrt{2\pi}e^2\ell_B}{4\pi\epsilon}I_0(\ell_B^2\boldsymbol{p}^2/4)e^{-\ell_B^2\boldsymbol{p}^2/4}, \tag{15}$$

with $V_X = V_X^+ + V_X^-$, $\quad V_X^d = V_X^+ - V_X^-$, and

$$V_D^\pm(\boldsymbol{p}) = \frac{e^2}{8\pi\epsilon|\boldsymbol{p}|}\left(1 \pm e^{-|\boldsymbol{p}|d}\right)e^{-\ell_B^2\boldsymbol{p}^2/2},$$

$$V_X^\pm(\boldsymbol{p}) = \frac{\sqrt{2\pi}e^2\ell_B}{8\pi\epsilon}I_0(\ell_B^2\boldsymbol{p}^2/4)e^{-\ell_B^2\boldsymbol{p}^2/4} \pm \frac{e^2\ell_B^2}{4\pi\epsilon}\int_0^\infty dk e^{-\frac{1}{2}\ell_B^2 k^2 - kd}J_0(\ell_B^2|\boldsymbol{p}|k). \tag{16}$$

Here, $I_0(x)$ is the modified Bessel function, and $J_0(x)$ is the Bessel function of the first kind.

Since the exchange interaction $V^\pm(\boldsymbol{p})$ is short ranged, it is a good approximation to make the derivative expansion, or, equivalently, the momentum expansion. We may set $\hat{\rho}^{\rm cl}(\boldsymbol{p}) = \rho_0$, $\hat{S}_a^{\rm cl}(\boldsymbol{p}) = \rho_\Phi\mathcal{S}_a(\boldsymbol{p})$, $\hat{P}_a^{\rm cl}(\boldsymbol{p}) = \rho_\Phi\mathcal{P}_a(\boldsymbol{p})$, and $\hat{R}_{ab}^{\rm cl}(\boldsymbol{p}) = \rho_\Phi\mathcal{R}_{ab}(\boldsymbol{p})$ for the study of NG modes. Taking the nontrivial lowest-order terms in the derivative expansion, we obtain the SU(4) effective Hamiltonian density

$$\mathcal{H}^{\rm eff} = J_s^d\left(\sum(\partial_k\mathcal{S}_a)^2 + (\partial_k\mathcal{P}_a)^2 + (\partial_k\mathcal{R}_{ab})^2\right) + 2J_s^-\left(\sum(\partial_k\mathcal{S}_a)^2 + (\partial_k\mathcal{P}_z)^2 + (\partial_k\mathcal{R}_{az})^2\right)$$

$$+ \rho_\phi\left[\epsilon_{\rm cap}(\mathcal{P}_z)^2 - 2\epsilon_X^-\left(\sum(\mathcal{S}_a)^2 + (\mathcal{R}_{az})^2\right) - (\Delta_{\rm Z}\mathcal{S}_z + \Delta_{\rm SAS}\mathcal{P}_x + \Delta_{\rm bias}\mathcal{P}_z)\right], \tag{17}$$

where $\rho_\Phi = \rho_0/\nu$ is the density of states, and

$$J_s = \frac{1}{16\sqrt{2\pi}}E_{\rm C}^0, \quad J_s^d = J_s\left[-\sqrt{\frac{2}{\pi}}\frac{d}{\ell_B} + \left(1 + \frac{d^2}{\ell_B^2}\right)e^{d^2/2\ell_B^2}{\rm erfc}\left(d/\sqrt{2}\ell_B\right)\right],$$

$$J_s^\pm = \frac{1}{2}(J_s \pm J_s^d),$$

$$\epsilon_X = \frac{1}{2}\sqrt{\frac{\pi}{2}}E_{\rm C}^0, \quad \epsilon_X^\pm = \frac{1}{2}\left[1 \pm e^{d^2/2\ell_B^2}{\rm erfc}\left(d/\sqrt{2}\ell_B\right)\right]\epsilon_X, \quad \epsilon_D^- = \frac{d}{4\ell_B}E_{\rm C}^0,$$

$$\epsilon_{\rm cap} = 4\epsilon_D^- - 2\epsilon_X^-, \tag{18}$$

with

$$E_{\rm C}^0 = \frac{e^2}{4\pi\epsilon\ell_B}. \tag{19}$$

This Hamiltonian is valid at $\nu = 1, 2$ and 3.

It should be noted that all potential terms vanish in the SU(4)-invariant limit, where perturbative excitations are gapless. They are the NG modes associated with spontaneous breaking of SU(4) symmetry. They get gapped in the actual system, since SU(4) symmetry is explicitly broken. Nevertheless, we call them the NG modes.

6

III. BILAYER QUANTUM HALL SYSTEM AT $\nu = 1$

In this section, we first show the ground state structure and the associated NG modes. We then show the interlayer phase coherence, the associated Josephson supercurrent, and its effect on the Hall resistance, in the limit $\Delta_{\text{SAS}} \to 0$.

A. Ground state structure

We introduce the CP^3 field based on the composite boson theory. An electron is converted into a composite boson by acquiring a flux quantum in the QH state. The CP^3 field emerges when composite bosons undergo Bose-Einstein condensation. The dimensionless SU(4) isospin densities are given by[3]:

$$
\begin{aligned}
\mathcal{S}_a(\boldsymbol{x}) &= \frac{1}{2}\boldsymbol{n}^\dagger \tau_a^{\text{spin}} \boldsymbol{n}, \\
\mathcal{P}_a(\boldsymbol{x}) &= \frac{1}{2}\boldsymbol{n}^\dagger \tau_a^{\text{ppin}} \boldsymbol{n}, \\
\mathcal{R}_{ab}(\boldsymbol{x}) &= \frac{1}{2}\boldsymbol{n}^\dagger \tau_a^{\text{spin}} \tau_b^{\text{ppin}} \boldsymbol{n},
\end{aligned}
\tag{20}
$$

where $\boldsymbol{n}$ is the CP^3 field of the form $\boldsymbol{n}(\boldsymbol{x}) = \left(n^{\text{f}\uparrow}, n^{\text{f}\downarrow}, n^{\text{b}\uparrow}, n^{\text{b}\downarrow}\right)^t$.

The ground state at the imbalanced configuration σ_0 is given by

$$
(n_g^{\text{B}\uparrow}, n_g^{\text{B}\downarrow}, n_g^{\text{A}\uparrow}, n_g^{\text{A}\downarrow}) = (1, 0, 0, 0),
\tag{21}
$$

in the bonding-antibonding representation, which reads

$$
\begin{pmatrix} n_g^{\text{f}\uparrow} \\ n_g^{\text{f}\downarrow} \\ n_g^{\text{b}\uparrow} \\ n_g^{\text{b}\downarrow} \end{pmatrix} = \frac{1}{\sqrt{2}} \begin{pmatrix} \sqrt{1+\sigma_0} & 0 & \sqrt{1-\sigma_0} & 0 \\ 0 & \sqrt{1+\sigma_0} & 0 & \sqrt{1-\sigma_0} \\ \sqrt{1-\sigma_0} & 0 & -\sqrt{1+\sigma_0} & 0 \\ 0 & \sqrt{1-\sigma_0} & 0 & -\sqrt{1+\sigma_0} \end{pmatrix} \begin{pmatrix} n_g^{\text{B}\uparrow} \\ n_g^{\text{B}\downarrow} \\ n_g^{\text{A}\uparrow} \\ n_g^{\text{A}\downarrow} \end{pmatrix} = \begin{pmatrix} \sqrt{\frac{1+\sigma_0}{2}} \\ 0 \\ \sqrt{\frac{1-\sigma_0}{2}} \\ 0 \end{pmatrix},
\tag{22}
$$

in the layer representation. The ground-state values of the isospin fields are

$$
\mathcal{S}_a^g = \frac{1}{2}\delta_{az}, \quad \mathcal{P}_a^g = \frac{1}{2}\left(\sqrt{1-\sigma_0^2}\delta_{ax} + \sigma_0\delta_{az}\right), \quad \mathcal{R}_{ab}^g = \frac{1}{2}\delta_{az}\left(\sqrt{1-\sigma_0^2}\delta_{bx} + \sigma_0\delta_{bz}\right), \tag{23}
$$

all others being zero, giving a unique phase. The residual symmetry keeping the ground state invariant is U(3). Thus, the symmetry-breaking pattern is SU(4)→U(3). The target space is the
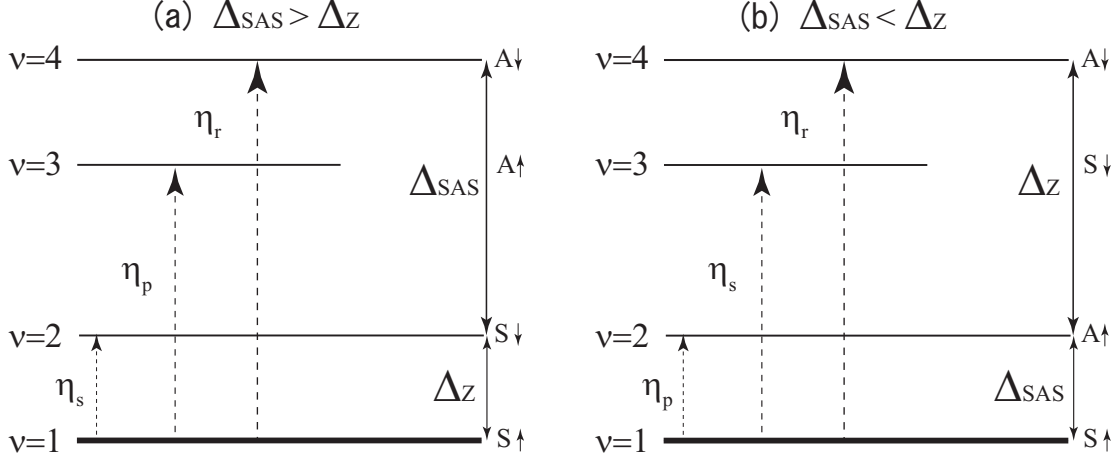
FIG. 1: The lowest Landau level contains four energy levels corresponding to the two layers and the two spin states. They are shown in (a) for $\Delta_{SAS} > \Delta_Z$ and (b) for $\Delta_{SAS} < \Delta_Z$. The lowest-energy level consists of up-spin symmetric states in the balanced configurations, and is filled at $\nu = 1$. It is the spin-ferromagnet and pseudospin-ferromagnet state. Small fluctuations are NG modes η_s, η_p, and η_r.

coset space

$$\mathrm{CP}^3 = \mathrm{SU}(4)/\mathrm{U}(3) = \mathrm{U}(4)/[\mathrm{U}(1) \otimes \mathrm{U}(3)], \tag{24}$$

which is the complex projective (CP) space.

B. Effective Hamiltonian for the NG modes at $\nu = 1$

From the previous subsection, we see that the symmetry-breaking pattern is given by (24), and therefore three complex NG modes emerge, which are described by the CP^3 fields.

We analyze the perturbative excitations around the ground state. We parameterize the bonding-antibonding state as

$$n^{B\uparrow} = \sqrt{1 - |\eta_s|^2 - |\eta_p|^2 - |\eta_r|^2}, \quad n^{B\downarrow} = \eta_s, \quad n^{A\uparrow} = \eta_p, \quad n^{A\downarrow} = \eta_r, \tag{25}$$

requiring the commutation relations

$$\left[\eta_i(\boldsymbol{x}), \eta_j^\dagger(\boldsymbol{y}) \right] = \rho_0^{-1} \delta_{ij} \delta(\boldsymbol{x} - \boldsymbol{y}), \tag{26}$$

8

in order to satisfy the SU(4) algebraic relation. $\eta_{\rm s}$ describes the spin wave, $\eta_{\rm p}$ the pseudospin wave, and $\eta_{\rm r}$ the R-spin wave connecting the ground state to the highest level in the lowest level (Fig. 1). The layer field reads

$$
\begin{pmatrix} n^{\rm f\uparrow} \\ n^{\rm f\downarrow} \\ n^{\rm b\uparrow} \\ n^{\rm b\downarrow} \end{pmatrix} = \frac{1}{\sqrt{2}} \begin{pmatrix} \sqrt{1+\sigma_0} & 0 & \sqrt{1-\sigma_0} & 0 \\ 0 & \sqrt{1+\sigma_0} & 0 & \sqrt{1-\sigma_0} \\ \sqrt{1-\sigma_0} & 0 & -\sqrt{1+\sigma_0} & 0 \\ 0 & \sqrt{1-\sigma_0} & 0 & -\sqrt{1+\sigma_0} \end{pmatrix} \begin{pmatrix} n^{\rm B\uparrow} \\ n^{\rm B\downarrow} \\ n^{\rm A\uparrow} \\ n^{\rm A\downarrow} \end{pmatrix}.
\tag{27}
$$

Expanding

$$
(n^{\rm B\uparrow}, n^{\rm B\downarrow}, n^{\rm A\uparrow}, n^{\rm A\downarrow}) = (1, \eta_{\rm s}, \eta_{\rm p}, \eta_{\rm r}) + \cdots,
\tag{28}
$$

for small fluctuations around the ground state, we obtain

$$
n^{\rm f\uparrow} = \sqrt{\frac{1+\sigma_0}{2}}\left(1 - \frac{1}{2}(|\eta_{\rm s}|^2 + |\eta_{\rm p}|^2 + |\eta_{\rm r}|^2)\right) + \eta_{\rm p}\sqrt{\frac{1-\sigma_0}{2}}, \quad n^{\rm f\downarrow} = \eta_{\rm s}\sqrt{\frac{1+\sigma_0}{2}} + \eta_{\rm r}\sqrt{\frac{1-\sigma_0}{2}},
$$
$$
n^{\rm b\uparrow} = \sqrt{\frac{1-\sigma_0}{2}}\left(1 - \frac{1}{2}(|\eta_{\rm s}|^2 + |\eta_{\rm p}|^2 + |\eta_{\rm r}|^2)\right) - \eta_{\rm p}\sqrt{\frac{1+\sigma_0}{2}}, \quad n^{\rm b\downarrow} = \eta_{\rm s}\sqrt{\frac{1-\sigma_0}{2}} - \eta_{\rm r}\sqrt{\frac{1+\sigma_0}{2}}.
\tag{29}
$$

We then set

$$
\eta_i(\boldsymbol{x}) = \frac{\sigma_i(\boldsymbol{x}) + i\vartheta_i(\boldsymbol{x})}{2},
\tag{30}
$$

where $\rho_0\sigma_i(\boldsymbol{x})$ is the number density excited from the ground state to the ith level designated by (29), and $\vartheta_i(\boldsymbol{x})$ is the conjugate phase field, satisfying the commutation relation

$$
\frac{\rho_0}{2}\left[\sigma_i(\boldsymbol{x}), \vartheta_j(\boldsymbol{y})\right] = i\delta_{ij}\delta(\boldsymbol{x}-\boldsymbol{y}).
\tag{31}
$$

We express the isospin field in terms of the CP^3 field (29),

$$
2\mathcal{S}_a = \left(\sigma_{\rm s} + \frac{1}{2}(\sigma_{\rm p}\sigma_{\rm r} + \vartheta_{\rm p}\vartheta_{\rm r}), \vartheta_{\rm s} + \frac{1}{2}(\sigma_{\rm p}\vartheta_{\rm r} - \vartheta_{\rm p}\sigma_{\rm r}), 1 - 2|\eta_{\rm s}|^2 - 2|\eta_{\rm r}|^2\right),
$$
$$
2\mathcal{P}_a = \left(p_x({\rm s}, {\rm p}, {\rm r}), -\vartheta_{\rm p} - \frac{1}{2}(\sigma_{\rm s}\vartheta_{\rm r} - \vartheta_{\rm s}\sigma_{\rm r}), p_z({\rm s}, {\rm p}, {\rm r})\right),
$$
$$
2\mathcal{R}_{xa} = \left(r_{xx}({\rm s}, {\rm p}, {\rm r}), -\vartheta_{\rm r} + \frac{1}{2}(\sigma_{\rm p}\vartheta_{\rm s} - \vartheta_{\rm p}\sigma_{\rm s}), r_{xz}({\rm s}, {\rm p}, {\rm r})\right),
$$
$$
2\mathcal{R}_{ya} = \left(r_{yx}({\rm s}, {\rm p}, {\rm r}), \sigma_{\rm r} - \frac{1}{2}(\sigma_{\rm s}\sigma_{\rm p} + \vartheta_{\rm s}\vartheta_{\rm p}), r_{yz}({\rm s}, {\rm p}, {\rm r})\right),
$$
$$
2\mathcal{R}_{za} = \left(r_{zy}({\rm s}, {\rm p}, {\rm r}), -\vartheta_{\rm p} + \frac{1}{2}(\sigma_{\rm s}\vartheta_{\rm r} - \vartheta_{\rm s}\sigma_{\rm r}), r_{zz}({\rm s}, {\rm p}, {\rm r})\right),
\tag{32}
$$

with

$$p_x(\mathrm{s},\mathrm{p},\mathrm{r}) = \sqrt{1-\sigma_0^2} - \sigma_0\sigma_\mathrm{p} - 2\sqrt{1-\sigma_0^2}\left(|\eta_\mathrm{p}|^2 + |\eta_\mathrm{r}|^2\right) - \frac{\sigma_0}{2}(\sigma_\mathrm{s}\sigma_\mathrm{r} + \vartheta_\mathrm{s}\vartheta_\mathrm{r}),$$

$$p_z(\mathrm{s},\mathrm{p},\mathrm{r}) = \sigma_0 + \sqrt{1-\sigma_0^2}\sigma_\mathrm{p} - 2\sigma_0\left(|\eta_\mathrm{p}|^2 + |\eta_\mathrm{r}|^2\right) + \frac{\sqrt{1-\sigma_0^2}}{2}(\sigma_\mathrm{s}\sigma_\mathrm{r} + \vartheta_\mathrm{s}\vartheta_\mathrm{r}),$$

$$r_{xx}(\mathrm{s},\mathrm{p},\mathrm{r}) = \sqrt{1-\sigma_0^2}\sigma_\mathrm{s} - \sigma_0\sigma_\mathrm{r} - \frac{\sigma_0}{2}\left(\sigma_\mathrm{s}\sigma_\mathrm{p} + \vartheta_\mathrm{s}\vartheta_\mathrm{p}\right) - \frac{\sqrt{1-\sigma_0^2}}{2}\left(\sigma_\mathrm{p}\sigma_\mathrm{r} + \vartheta_\mathrm{p}\vartheta_\mathrm{r}\right),$$

$$r_{yx}(\mathrm{s},\mathrm{p},\mathrm{r}) = \sqrt{1-\sigma_0^2}\vartheta_\mathrm{s} - \sigma_0\vartheta_\mathrm{r} + \frac{\sigma_0}{2}\left(\sigma_\mathrm{s}\vartheta_\mathrm{p} - \vartheta_\mathrm{s}\sigma_\mathrm{p}\right) - \frac{\sqrt{1-\sigma_0^2}}{2}\left(\sigma_\mathrm{p}\vartheta_\mathrm{r} - \vartheta_\mathrm{p}\sigma_\mathrm{r}\right),$$

$$r_{xz}(\mathrm{s},\mathrm{p},\mathrm{r}) = \sigma_0\sigma_\mathrm{s} + \sqrt{1-\sigma_0^2}\sigma_\mathrm{r} - \frac{\sigma_0}{2}\left(\sigma_\mathrm{p}\sigma_\mathrm{r} + \vartheta_\mathrm{p}\vartheta_\mathrm{r}\right) + \frac{\sqrt{1-\sigma_0^2}}{2}\left(\sigma_\mathrm{s}\sigma_\mathrm{p} + \vartheta_\mathrm{s}\vartheta_\mathrm{p}\right),$$

$$r_{yz}(\mathrm{s},\mathrm{p},\mathrm{r}) = \sigma_0\vartheta_\mathrm{s} + \sqrt{1-\sigma_0^2}\vartheta_\mathrm{r} - \frac{\sigma_0}{2}\left(\sigma_\mathrm{p}\vartheta_\mathrm{r} - \vartheta_\mathrm{p}\sigma_\mathrm{r}\right) - \frac{\sqrt{1-\sigma_0^2}}{2}\left(\sigma_\mathrm{s}\vartheta_\mathrm{p} - \vartheta_\mathrm{s}\sigma_\mathrm{p}\right),$$

$$r_{zx}(\mathrm{s},\mathrm{p},\mathrm{r}) = \sqrt{1-\sigma_0^2} - \sigma_0\sigma_\mathrm{p} - 2\sqrt{1-\sigma_0^2}\left(|\eta_\mathrm{p}|^2 + |\eta_\mathrm{s}|^2\right) + \frac{\sigma_0}{2}(\sigma_\mathrm{s}\sigma_\mathrm{r} + \vartheta_\mathrm{s}\vartheta_\mathrm{r}),$$

$$r_{zz}(\mathrm{s},\mathrm{p},\mathrm{r}) = \sigma_0 + \sqrt{1-\sigma_0^2}\sigma_\mathrm{p} - 2\sigma_0\left(|\eta_\mathrm{p}|^2 + |\eta_\mathrm{s}|^2\right) - \frac{\sqrt{1-\sigma_0^2}}{2}(\sigma_\mathrm{s}\sigma_\mathrm{r} + \vartheta_\mathrm{s}\vartheta_\mathrm{r}). \tag{33}$$

Substituting these into (17), we obtain the effective Hamiltonian

$$\int d^2k\mathcal{H}_\mathrm{eff} = \int d^2k\mathcal{H}_\mathrm{ppin} + \int d^2k\mathcal{H}_\mathrm{mix}, \tag{34}$$

with

$$\mathcal{H}_\mathrm{ppin} = \frac{(1-\sigma_0^2)J_s + \sigma_0^2 J_s^d}{2}(\partial_k\sigma_\mathrm{p})^2 + \frac{\rho_0}{4}\left[\epsilon_\mathrm{cap}^{\nu=1}(1-\sigma_0^2) + \frac{\Delta_\mathrm{SAS}}{\sqrt{1-\sigma_0^2}}\right]\sigma_\mathrm{p}^2$$

$$+ \frac{1}{2}J_s^d(\partial_k\vartheta_\mathrm{p})^2 + \frac{\rho_0}{4}\frac{\Delta_\mathrm{SAS}}{\sqrt{1-\sigma_0^2}}\vartheta_\mathrm{p}^2, \tag{35}$$

$$\mathcal{H}_\mathrm{mix} = \frac{J_s^+ + \sigma_0 J_s^-}{2}\left[(\partial_k\sigma_1)^2 + (\partial_k\vartheta_1)^2\right] + \frac{\rho_0}{4}\left(\Delta_\mathrm{Z} + \frac{1}{2}\Delta_\mathrm{SAS}\frac{\sqrt{1-\sigma_0}}{\sqrt{1+\sigma_0}}\right)\left[\sigma_1^2 + \vartheta_1^2\right]$$

$$+ \frac{J_s^+ - \sigma_0 J_s^-}{2}\left[(\partial_k\sigma_2)^2 + (\partial_k\vartheta_2)^2\right] + \frac{\rho_0}{4}\left(\Delta_\mathrm{Z} + \frac{1}{2}\Delta_\mathrm{SAS}\frac{\sqrt{1-\sigma_0}}{\sqrt{1+\sigma_0}}\right)\left[\sigma_2^2 + \vartheta_2^2\right]$$

$$- \frac{\rho_0}{4}\Delta_\mathrm{SAS}(\sigma_1\sigma_2 + \vartheta_1\vartheta_2), \tag{36}$$

where we change the variables in (36) as

$$\eta_\mathrm{s} = \sqrt{\frac{1+\sigma_0}{2}}\eta_1 + \sqrt{\frac{1-\sigma_0}{2}}\eta_2, \quad \eta_\mathrm{r} = \sqrt{\frac{1-\sigma_0}{2}}\eta_1 - \sqrt{\frac{1+\sigma_0}{2}}\eta_2, \tag{37}$$

and Δ_bias and $\epsilon_\mathrm{cap}^{\nu=1}$ are given by

$$\Delta_\mathrm{bias} = \frac{\sigma_0}{\sqrt{1-\sigma_0^2}}\Delta_\mathrm{SAS} + \sigma_0\epsilon_\mathrm{cap}^{\nu=1}, \tag{38}$$

$$\epsilon_\mathrm{cap}^{\nu=1} = 4(\epsilon_D^- - \epsilon_X^-), \tag{39}$$

10

respectively. The pseudospin mode is decoupled from other modes, and from (35) we have coherence lengths of the interlayer phase field ϑ_p and the imbalanced field σ_p

$$
\xi^\vartheta_\mathrm{ppin} = 2l_B\sqrt{\frac{\pi\sqrt{1-\sigma_0^2}\,J_s^d}{\Delta_\mathrm{SAS}}},
$$

$$
\xi^\sigma_\mathrm{ppin} = 2l_B\sqrt{\frac{\pi\left[(1-\sigma_0^2)J_s + \sigma_0^2 J_s^d\right]}{\epsilon_\mathrm{cap}^{\nu=1}(1-\sigma_0^2) + \Delta_\mathrm{SAS}/\sqrt{1-\sigma_0^2}}}. \tag{40}
$$

The ϑ_p mode is gapless for $\Delta_\mathrm{SAS} = 0$, though the σ_p mode is gapful due to the capacitance term $\epsilon_\mathrm{cap}^{\nu=1}$.

On the other hand, from (36) for $\Delta_\mathrm{SAS} = 0$, the two modes η_1 and η_2 are decoupled. There exist no gapless modes in the Hamiltonian (36) provided $\Delta_\mathrm{Z} \neq 0$.

C. Effective Hamiltonian for the NG modes in the limit $\Delta_\mathrm{SAS} \to 0$

We concentrate solely on the gapless mode in the limit $\Delta_\mathrm{SAS} \to 0$, since we are interested in the interlayer coherence in this system. We now analyze the nonperturbative phase-coherent phenomena, where the phase field $\vartheta(\boldsymbol{x})$ is essentially classical and may become very large. We parameterize the CP^3 field as

$$
\begin{pmatrix} n^{\mathrm{f}\uparrow}(\boldsymbol{x}) \\ n^{\mathrm{f}\downarrow}(\boldsymbol{x}) \\ n^{\mathrm{b}\uparrow}(\boldsymbol{x}) \\ n^{\mathrm{b}\downarrow}(\boldsymbol{x}) \end{pmatrix} = \frac{1}{\sqrt{2}}\begin{pmatrix} e^{i\vartheta(\boldsymbol{x})/2}\sqrt{1+\sigma(\boldsymbol{x})} \\ 0 \\ e^{-i\vartheta(\boldsymbol{x})/2}\sqrt{1-\sigma(\boldsymbol{x})} \\ 0 \end{pmatrix}. \tag{41}
$$

Then the isospin fields are expressed as

$$
\mathcal{S}_z(\boldsymbol{x}) = \frac{1}{2}, \quad \mathcal{P}_z(\boldsymbol{x}) = \mathcal{R}_{zz}(\boldsymbol{x}) = \frac{1}{2}\sigma(\boldsymbol{x}),
$$

$$
\mathcal{P}_x(\boldsymbol{x}) = \mathcal{R}_{zx}(\boldsymbol{x}) = \frac{1}{2}\sqrt{1-\sigma^2(\boldsymbol{x})}\cos\vartheta(\boldsymbol{x}), \quad \mathcal{P}_y(\boldsymbol{x}) = \mathcal{R}_{zy}(\boldsymbol{x}) = -\frac{1}{2}\sqrt{1-\sigma^2(\boldsymbol{x})}\sin\vartheta(\boldsymbol{x}),
$$

$$
\tag{42}
$$

with all others being zero. From (42) we obtain the effective Hamiltonian

$$
\mathcal{H}_\mathrm{eff} = \frac{J_s^d}{2}(1-\sigma^2(\boldsymbol{x}))(\partial_k\vartheta(\boldsymbol{x}))^2 + \frac{1}{2}\left(J_s + \frac{\sigma^2(\boldsymbol{x})}{1-\sigma^2(\boldsymbol{x})}J_s^d\right)(\partial_k\sigma(\boldsymbol{x}))^2
$$

$$
+ \frac{\rho_0\epsilon_\mathrm{cap}^{\nu=1}}{4}(\sigma(\boldsymbol{x})-\sigma_0)^2 - \frac{\rho_0\Delta_\mathrm{SAS}}{2}\left(\sqrt{1-\sigma^2(\boldsymbol{x})}\cos\vartheta(\boldsymbol{x}) + \frac{\sigma_0}{\sqrt{1-\sigma_0^2}}\sigma(\boldsymbol{x})\right). \tag{43}
$$

11

The canonical commutation relation is given by

$$\frac{\rho_0}{2}\left[\sigma(\boldsymbol{x}), \vartheta(\boldsymbol{x})\right] = i\delta(\boldsymbol{x} - \boldsymbol{y}). \tag{44}$$

From (43) and (44), the Heisenberg equations of motion can be calculated as

$$\hbar\partial_t\vartheta = \frac{2}{\rho_0}\partial_k(J_{\mathrm{s}}^\sigma\partial_k\sigma) + \frac{2J_s^d}{\rho_0}\sigma\left[(\partial_k\vartheta)^2 - \frac{1}{1-\sigma^2}(\partial_k\sigma)^2\right]$$
$$- \epsilon_{\mathrm{cap}}^{\nu=1}(\sigma - \sigma_0) - \frac{\sigma\cos\vartheta}{\sqrt{1-\sigma^2}}\Delta_{\mathrm{SAS}} + \frac{\sigma_0}{\sqrt{1-\sigma_0^2}}\Delta_{\mathrm{SAS}}, \tag{45}$$

$$\hbar\partial_t\sigma = -\frac{2}{\rho_0}\partial_k(J_{\mathrm{s}}^\vartheta\partial_k\vartheta) + \Delta_{\mathrm{SAS}}\sqrt{1-\sigma^2}\sin\vartheta, \tag{46}$$

with

$$J_{\mathrm{s}}^\vartheta = (1-\sigma^2)J_s^d, \quad J_{\mathrm{s}}^\sigma = J_s + \frac{\sigma^2}{1-\sigma^2}J_s^d. \tag{47}$$

D.   Josephson supercurrents

We now study the electric Josephson supercurrent carried by the gapless mode $\vartheta(\boldsymbol{x})$. In general, the total current consists of three types of current, the Josephson in-plane current $\mathcal{J}_i^{\mathrm{Jos}}$, the Josephson tunneling current $\mathcal{J}_z^{\mathrm{Jos}}$, which is proportional to Δ_{SAS}, and the Hall current $\mathcal{J}_i^{\mathrm{Hall}}$. What has been argued in [13] is that in the case of $\nu = 1$, there exists an interlayer voltage V_{junc} and thus no dissipationless $\mathcal{J}_z^{\mathrm{Jos}}$ exists, when $\sigma_0 \neq 0$. On the other hand, the Josephson in-plane current, which is dissipationless does exist, even for $\sigma_0 \neq 0$. Here, we assume the sample parameter $\sigma_0 \neq 0$ and $\Delta_{\mathrm{SAS}} = 0$ so that there is no dissipationless tunneling current $\mathcal{J}_z^{\mathrm{Jos}}$ between the two layers.

The electron densities are $\rho_e^{\mathrm{f(b)}} = -e\rho_0\left(1/2 \pm \mathcal{P}_z\right) = -e\rho_0\left(1 \pm \sigma(\boldsymbol{x})\right)/2$ on each layer. Taking the time derivative and using (46) we find

$$\partial_t\rho_e^{\mathrm{f}} = -\partial_t\rho_e^{\mathrm{b}} = \frac{eJ_{\mathrm{s}}^\vartheta}{\hbar}\nabla^2\vartheta(\boldsymbol{x}). \tag{48}$$

The time derivative of the charge is associated with the current via the continuity equation, $\partial_t\rho_e^{\mathrm{f(b)}} = \partial_i\mathcal{J}_i^{\mathrm{f(b)}}$. We thus identify $\mathcal{J}_i^{\mathrm{f(b)}} = \pm\mathcal{J}_i^{\mathrm{Jos}}(\boldsymbol{x})+$constant, where

$$\mathcal{J}_i^{\mathrm{Jos}}(\boldsymbol{x}) \equiv \frac{eJ_{\mathrm{s}}^\vartheta}{\hbar}\partial_i\vartheta(\boldsymbol{x}). \tag{49}$$

Consequently, the current $\mathcal{J}_i^{\mathrm{Jos}}(\boldsymbol{x})$ flows when there exists inhomogeneity in the phase $\vartheta(\boldsymbol{x})$. Such a current is precisely the Josephson supercurrent. Indeed, it is a supercurrent because the coherent mode exhibits a linear dispersion relation.

12

E. Quantum Hall effects

Let us inject the current $\mathcal{J}_{\mathrm{in}}$ into the x direction of the bilayer sample, and assume the system to be homogeneous in the y direction (Fig.2). This creates the electric field $E_y^{\mathrm{f(b)}}$ so that the Hall current flows into the x-direction. A bilayer system consists of the two layers and the volume between them. The Coulomb energy in the volume is minimized[12] by the condition $E_y^{\mathrm{f}} = E_y^{\mathrm{b}}$. We thus impose $E_y^{\mathrm{f}} = E_y^{\mathrm{b}} \equiv E_y$. The current is the sum of the Hall current and the Josephson current,

$$\mathcal{J}_x^{\mathrm{f}}(x) = \frac{\nu}{R_{\mathrm{K}}} \frac{\rho_0^{\mathrm{f}}}{\rho_0} E_y + \mathcal{J}_x^{\mathrm{Jos}}, \quad \mathcal{J}_x^{\mathrm{b}}(x) = \frac{\nu}{R_{\mathrm{K}}} \frac{\rho_0^{\mathrm{b}}}{\rho_0} E_y - \mathcal{J}_x^{\mathrm{Jos}}, \tag{50}$$

with $R_{\mathrm{K}} = 2\pi\hbar/e^2$ the von Klitzing constant. We obtain the standard Hall resistance when $\mathcal{J}_x^{\mathrm{Jos}} = 0$. That is, the emergence of the Josephson supercurrent is detected if the Hall resistance becomes anomalous.

We apply these formulas to analyze the counterflow and drag experiments since they occur without tunneling. In the counterflow experiment, the current $\mathcal{J}_{\mathrm{in}}$ is injected to the front layer and extracted from the back layer at the same edge. Since there is no tunneling we have $\mathcal{J}_x^{\mathrm{b}} = -\mathcal{J}_x^{\mathrm{f}} = -\mathcal{J}_{\mathrm{in}}$. Hence, it follows from (50) that $E_y = 0$, or

$$R_{xy}^{\mathrm{f}} \equiv \frac{E_y^{\mathrm{f}}}{\mathcal{J}_x^{\mathrm{f}}} = 0, \qquad R_{xy}^{\mathrm{b}} \equiv \frac{E_y^{\mathrm{b}}}{\mathcal{J}_x^{\mathrm{b}}} = 0. \tag{51}$$

All the input current is carried by the Josephson supercurrent, $\mathcal{J}_x^{\mathrm{Jos}} = \mathcal{J}_{\mathrm{in}}$. It generates such an inhomogeneous phase field that $\vartheta(\boldsymbol{x}) = (\hbar/eJ_s^\vartheta)\mathcal{J}_{\mathrm{in}}x$.

On the other hand, in the drag experiment, since interlayer-coherent tunneling is absent, no current flows on the back layer, or $\mathcal{J}_x^{\mathrm{b}} = 0$. Hence, it follows from (50) that $\mathcal{J}_{\mathrm{in}} = \mathcal{J}_x^{\mathrm{f}} = (\nu/R_{\mathrm{K}})E_y$, or

$$R_{xy}^{\mathrm{f}} \equiv \frac{E_y^{\mathrm{f}}}{\mathcal{J}_x^{\mathrm{f}}} = \frac{R_{\mathrm{K}}}{\nu}, \tag{52}$$

A part of the input current is carried by the Josephson supercurrent, $\mathcal{J}_x^{\mathrm{Jos}} = \frac{1}{2}(1 - \sigma_0)\mathcal{J}_{\mathrm{in}}$.
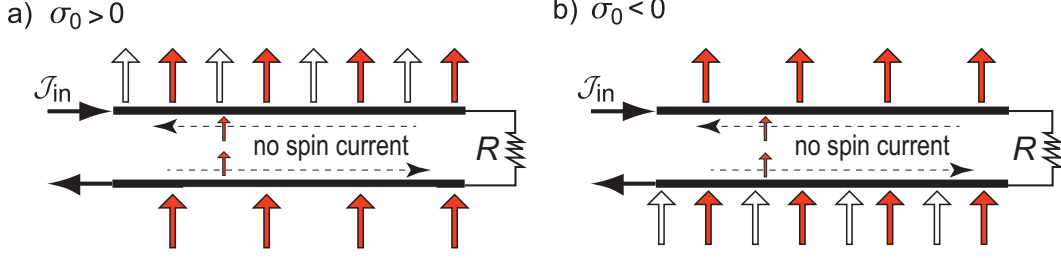
FIG. 2: Schematic illustration of the spin supercurrent flowing along the x axis in the counterflow geometry for $\nu = 1$ bilayer QH system. (a) In the $\nu = 1$ bilayer QH system for $\sigma_0 > 0$, all spins are polarized into the positive z axis. The interlayer phase difference $\vartheta(\boldsymbol{x})$ is created by feeding a charge current $\mathcal{J}_{\text{in}}$ to the front layer, which also drives the spin current. Electrons flow in each layer as indicated by the dotted horizontal arrows. The direction of the spin current flowing in the front layer becomes opposite to the direction of that flowing in the back layer, and therefore no spin current flows as a whole. (b) In the $\nu = 1$ QH bilayer system for $\sigma_0 < 0$, similar phenomena occur and therefore no spin current flows as a whole.

F. Spin Josephson supercurrents

The spin density in each layer is defined by $\rho_\alpha^{\text{spin}}(\boldsymbol{x}) \equiv s_\alpha \psi_\alpha^\dagger \psi_\alpha$, where $s_\alpha = \frac{1}{2}\hbar$ for $\alpha = \text{f}\uparrow, \text{b}\uparrow$ and $s_\alpha = -\frac{1}{2}\hbar$ for $\alpha = \text{f}\downarrow, \text{b}\downarrow$. By using the formula

$$
\begin{pmatrix}
\rho_{\text{f}\uparrow}(\boldsymbol{x}) \\
\rho_{\text{f}\downarrow}(\boldsymbol{x}) \\
\rho_{\text{b}\uparrow}(\boldsymbol{x}) \\
\rho_{\text{b}\downarrow}(\boldsymbol{x})
\end{pmatrix}
= \frac{1}{4}
\begin{pmatrix}
1 & 1 & 1 & 1 \\
1 & -1 & 1 & -1 \\
1 & 1 & -1 & -1 \\
1 & -1 & -1 & 1
\end{pmatrix}
\begin{pmatrix}
\rho_0 \\
2S_z(\boldsymbol{x}) \\
2P_z(\boldsymbol{x}) \\
2R_{zz}(\boldsymbol{x})
\end{pmatrix},
\tag{53}
$$

and (42) we have

$$
\begin{pmatrix}
\rho_{\text{f}\uparrow}(\boldsymbol{x}) \\
\rho_{\text{f}\downarrow}(\boldsymbol{x}) \\
\rho_{\text{b}\uparrow}(\boldsymbol{x}) \\
\rho_{\text{b}\downarrow}(\boldsymbol{x})
\end{pmatrix}
= \frac{\rho_0}{2}
\begin{pmatrix}
1 + \sigma(\boldsymbol{x}) \\
0 \\
1 - \sigma(\boldsymbol{x}) \\
0
\end{pmatrix}.
\tag{54}
$$

14

Then taking the time derivative for ρ_α, we have

$$
\begin{pmatrix}
\partial_t \rho_{\text{f}\uparrow}^{\text{spin}}(\boldsymbol{x}) \\
\partial_t \rho_{\text{f}\downarrow}^{\text{spin}}(\boldsymbol{x}) \\
\partial_t \rho_{\text{b}\uparrow}^{\text{spin}}(\boldsymbol{x}) \\
\partial_t \rho_{\text{b}\downarrow}^{\text{spin}}(\boldsymbol{x})
\end{pmatrix}
= \frac{\hbar \rho_0}{4}
\begin{pmatrix}
\partial_t \sigma(\boldsymbol{x}) \\
0 \\
-\partial_t \sigma(\boldsymbol{x}) \\
0
\end{pmatrix}.
\tag{55}
$$

The time derivative of the spin is associated with the spin current via the continuity equation (in this article we neglect the tunneling current):

$$
\partial_t \rho_\alpha^{\text{Spin}}(\boldsymbol{x}) = \partial_x \mathcal{J}_\alpha^{\text{Spin}}(\boldsymbol{x}),
\tag{56}
$$

for each α. We thus identify

$$
\mathcal{J}_{\text{f}\uparrow}^{\text{Spin}}(\boldsymbol{x}) = -\mathcal{J}_{\text{b}\uparrow}^{\text{Spin}}(\boldsymbol{x}) = -\frac{J_s^\vartheta}{2}\partial_x \vartheta(\boldsymbol{x}), \quad \text{all others} = 0.
\tag{57}
$$

Therefore from (57) we see that the total spin current $\mathcal{J}^{\text{Spin}} \equiv \sum_\alpha \mathcal{J}_\alpha^{\text{Spin}}$ is zero, and therefore the spin Josephson supercurrent does not flow at $\nu = 1$ (Fig. 2).

IV.   BILAYER QUANTUM HALL SYSTEM AT $\nu = 2$

The standard Hall resistance is given by $R_{xy}^{\text{f}} = \frac{2}{\nu}R_{\text{K}} = R_{\text{K}}$ at $\nu = 2$. On the other hand, it has been found experimentally [8–10] that $R_{xy}^{\text{f}} = R_{\text{K}}$ at $\nu = 2$. It seems that the interlayer phase coherence together with the supercurrent does not develop at $\nu = 2$. Note that the experiments [8–10] were performed at the balance point $\sigma_0 = 0$. As we now demonstrate, the interlayer phase coherence develops only at the imbalance point $\sigma_0 \neq 0$ in the CAF phase.

In this section, we first show the ground state structure and the NG modes for each phase. We then discuss the entangled spin-pseudospin phase coherence, the associated Josephson supercurrent and its effect on the Hall resistance in the CAF phase in the limit $\Delta_{\text{SAS}} \to 0$.

A. Ground state structure

It has been shown[22] at $\nu = 2$ that the order parameters, which are the classical isospin densities for the ground state, are given in terms of two parameters α and β as

$$\mathcal{S}_z^0 = \frac{\Delta_Z}{\Delta_0}(1 - \alpha^2)\sqrt{1 - \beta^2}, \quad \mathcal{P}_x^0 = \frac{\Delta_{SAS}}{\Delta_0}\alpha^2\sqrt{1 - \beta^2}, \quad \mathcal{P}_z^0 = \frac{\Delta_{SAS}}{\Delta_0}\alpha^2\beta,$$

$$\mathcal{R}_{xx}^0 = -\frac{\Delta_{SAS}}{\Delta_0}\alpha\sqrt{1 - \alpha^2}\beta, \quad \mathcal{R}_{yy}^0 = -\frac{\Delta_Z}{\Delta_0}\alpha\sqrt{1 - \alpha^2}\sqrt{1 - \beta^2}, \quad \mathcal{R}_{xz}^0 = \frac{\Delta_{SAS}}{\Delta_0}\alpha\sqrt{1 - \alpha^2}\sqrt{1 - \beta^2},$$

$$\tag{58}$$

with all others being zero. The parameters α and β, satisfying $|\alpha| \leq 1$ and $|\beta| \leq 1$, are determined by the variational equations as

$$\Delta_Z^2 = \frac{\Delta_{SAS}^2}{1 - \beta^2} - \frac{4\epsilon_X^- (\Delta_0^2 - \beta^2\Delta_{SAS}^2)}{\Delta_0\sqrt{1 - \beta^2}}, \tag{59}$$

$$\frac{\Delta_{bias}}{\beta\Delta_{SAS}} = \frac{4\left(\epsilon_X^- + 2\alpha^2(\epsilon_D^- - \epsilon_X^-)\right)}{\Delta_0} + \frac{1}{\sqrt{1 - \beta^2}}, \tag{60}$$

where

$$\Delta_0 = \sqrt{\Delta_{SAS}^2\alpha^2 + \Delta_Z^2(1 - \alpha^2)(1 - \beta^2)}. \tag{61}$$

As a physical variable it is more convenient to use the imbalance parameter defined by

$$\sigma_0 \equiv \mathcal{P}_z^0 = \frac{\Delta_{SAS}}{\Delta_0}\alpha^2\beta, \tag{62}$$

instead of the bias voltage Δ_{bias}. This is possible in the pseudospin and CAF phases. The bilayer system is balanced at $\sigma_0 = 0$, while all electrons are in the front layer at $\sigma_0 = 1$, and in the back layer at $\sigma_0 = -1$.

There are three phases in the bilayer QH system at $\nu = 2$. We discuss them in terms of α and β.

First, when $\alpha = 0$, it follows that $\mathcal{S}_z^0 = 1$, $\mathcal{P}_a^0 = \mathcal{R}_{ab}^0 = 0$, since $\Delta_0 = \Delta_Z\sqrt{1 - \beta^2}$. Note that β disappears from all formulas in (58). This is the spin phase, which is characterized by the fact that the isospin is fully polarized into the spin direction with

$$\mathcal{S}_z^0 = 1, \tag{63}$$

all others being zero. The spins in both layers point to the positive z axis due to the Zeeman effect.

Second, when $\alpha = 1$, it follows that $\mathcal{S}_z^0 = 0$ and $(\mathcal{P}_x^0)^2 + (\mathcal{P}_z^0)^2 = 1$. This is the pseudospin phase, which is characterized by the fact that the isospin is fully polarized into the pseudospin

16

direction with

$$\mathcal{P}_x^0 = \sqrt{1-\beta^2}, \qquad \mathcal{P}_z^0 = \beta = \sigma_0, \tag{64}$$

all the others being zero.

For intermediate values of α $(0 < \alpha < 1)$, not only the spin and pseudospin but also some components of the residual spin are nonvanishing, and we may control the density imbalance by applying a bias voltage as in the pseudospin phase. It follows from (58) that, as the system goes away from the spin phase $(\alpha = 0)$, the spins begin to cant coherently and make antiferromagnetic correlations between the two layers. Hence it is called the canted antiferromagnetic phase.

The interlayer phase coherence is an intriguing phenomenon in the bilayer QH system[3]. Since it is enhanced in the limit $\Delta_{\mathrm{SAS}} \to 0$, it is interesting to also investigate the effective Hamiltonian in this limit at $\nu = 2$. We need to know how the parameters α and β are expressed in terms of the physical variables. The solutions for (61) are

$$\beta = \pm\sqrt{1 - \left(\frac{\Delta_{\mathrm{SAS}}}{\Delta_{\mathrm{Z}}}\right)^2} + O(\Delta_{\mathrm{SAS}}^4), \tag{65}$$

with

$$\Delta_0 \to \Delta_{\mathrm{SAS}} + O(\Delta_{\mathrm{SAS}}^3), \tag{66}$$

as we shall derive in (157). By using (62) we have

$$\mathcal{P}_z^0 = \sigma_0 = \pm\alpha^2 + O(\Delta_{\mathrm{SAS}}^2). \tag{67}$$

The parameters α and β are simple functions of the physical variables $\Delta_{\mathrm{SAS}}/\Delta_{\mathrm{Z}}$ and σ_0 in the limit $\Delta_{\mathrm{SAS}} \to 0$.

In particular, one of the layers becomes empty in the pseudospin phase and also near the pseudospin phase boundary in the CAF phase, since we have $\sigma_0 \to \pm 1$ as $\alpha \to 1$. On the other hand, the bilayer system becomes balanced in the spin phase and also near the spin phase boundary in the CAF phase, since we have $\sigma_0 \to 0$ as $\alpha \to 0$.

B. Grassmannian approach

We employ the Grassmannian formalism[18] to make the physical picture of this NG mode clearer and to construct a theory which is valid nonperturbatively. The Grassmannian field $Z(\boldsymbol{x})$ consists of two CP^3 fields $\boldsymbol{n}_1(\boldsymbol{x})$ and $\boldsymbol{n}_2(\boldsymbol{x})$ at $\nu = 2$, since there are two electrons per one Landau

17

site. Due to the Pauli exclusion principle they should be orthogonal one to another. Hence, we require

$$\boldsymbol{n}_i^\dagger(\boldsymbol{x}) \cdot \boldsymbol{n}_j(\boldsymbol{x}) = \delta_{ij}, \tag{68}$$

with $i = 1, 2$. Using a set of two CP^3 fields subject to this normalization condition we introduce a 4×2 matrix field, the Grassmannian field given by

$$Z(\boldsymbol{x}) = (\boldsymbol{n}_1, \boldsymbol{n}_2), \tag{69}$$

obeying

$$Z^\dagger Z = \mathbf{1}. \tag{70}$$

Though we have introduced two fields $\boldsymbol{n}_1(\boldsymbol{x})$ and $\boldsymbol{n}_2(\boldsymbol{x})$, we cannot distinguish them quantum mechanically since they describe two electrons in the same Landau site. Namely, two fields $Z(\boldsymbol{x})$ and $Z'(\boldsymbol{x})$ are indistinguishable physically when they are related by a local U(2) transformation $U(\boldsymbol{x})$,

$$Z'(\boldsymbol{x}) = Z(\boldsymbol{x})U(\boldsymbol{x}). \tag{71}$$

By identifying these two fields $Z(\boldsymbol{x})$ and $Z'(\boldsymbol{x})$, the 4×2 matrix field $Z(\boldsymbol{x})$ takes values on the Grassmann manifold $\mathrm{G}_{4,2}$ defined by

$$\mathrm{G}_{4,2} = \frac{\mathrm{SU}(4)}{\mathrm{U}(1) \otimes \mathrm{SU}(2) \otimes \mathrm{SU}(2)}. \tag{72}$$

The field $Z(\boldsymbol{x})$ is no longer a set of two independent CP^3 fields. It is a new object, called the Grassmannian field, carrying eight real degrees of freedom.

The dimensionless SU(4) isospin densities are given by

$$\mathcal{S}_a(\boldsymbol{x}) = \frac{1}{2}\mathrm{Tr}\left[Z^\dagger \tau_a^{\mathrm{spin}} Z\right] = \frac{1}{2}\sum_{i=1}^2 \boldsymbol{n}_i^\dagger \tau_a^{\mathrm{spin}} \boldsymbol{n}_i,$$

$$\mathcal{P}_a(\boldsymbol{x}) = \frac{1}{2}\mathrm{Tr}\left[Z^\dagger \tau_a^{\mathrm{ppin}} Z\right] = \frac{1}{2}\sum_{i=1}^2 \boldsymbol{n}_i^\dagger \tau_a^{\mathrm{ppin}} \boldsymbol{n}_i,$$

$$\mathcal{R}_{ab}(\boldsymbol{x}) = \frac{1}{2}\mathrm{Tr}\left[Z^\dagger \tau_a^{\mathrm{spin}} \tau_b^{\mathrm{ppin}} Z\right] = \frac{1}{2}\sum_{i=1}^2 \boldsymbol{n}_i^\dagger \tau_a^{\mathrm{spin}} \tau_b^{\mathrm{ppin}} \boldsymbol{n}_i, \tag{73}$$

where $\boldsymbol{n}_i$ consists of the basis $\boldsymbol{n}_i(\boldsymbol{x}) = \left(n^{\mathrm{f}\uparrow}, n^{\mathrm{f}\downarrow}, n^{\mathrm{b}\uparrow}, n^{\mathrm{b}\downarrow}\right)^t$. The ground state is given by Eq. (58), which we express in terms of the two CP^3 fields $\boldsymbol{n}_i^g$. It is straightforward to show that it is given

by $\boldsymbol{n}_i^g = U\bar{\boldsymbol{n}}_i^g$ with

$$U = \exp\left[-\frac{i}{2}\tau_y^{\mathrm{ppin}}(\theta_\beta + \frac{\pi}{2})\right]\exp\left[-\frac{i}{2}\tau_x^{\mathrm{spin}}\tau_y^{\mathrm{ppin}}\theta_\alpha\right]\exp\left[\frac{i}{2}\tau_y^{\mathrm{spin}}\tau_x^{\mathrm{ppin}}\theta_\delta\right]$$

$$= \begin{pmatrix} \cos\frac{(2\theta_\beta+\pi)}{4}\cos\frac{\theta_\delta-\theta_\alpha}{2} & -\sin\frac{(2\theta_\beta+\pi)}{4}\sin\frac{\theta_\delta+\theta_\alpha}{2} & -\sin\frac{(2\theta_\beta+\pi)}{4}\cos\frac{\theta_\delta+\theta_\alpha}{2} & \cos\frac{(2\theta_\beta+\pi)}{4}\sin\frac{\theta_\delta-\theta_\alpha}{2} \\ \sin\frac{(2\theta_\beta+\pi)}{4}\sin\frac{\theta_\delta-\theta_\alpha}{2} & \cos\frac{(2\theta_\beta+\pi)}{4}\cos\frac{\theta_\delta+\theta_\alpha}{2} & -\cos\frac{(2\theta_\beta+\pi)}{4}\sin\frac{\theta_\delta+\theta_\alpha}{2} & -\sin\frac{(2\theta_\beta+\pi)}{4}\cos\frac{\theta_\delta-\theta_\alpha}{2} \\ \sin\frac{(2\theta_\beta+\pi)}{4}\cos\frac{\theta_\delta-\theta_\alpha}{2} & \cos\frac{(2\theta_\beta+\pi)}{4}\sin\frac{\theta_\delta+\theta_\alpha}{2} & \cos\frac{(2\theta_\beta+\pi)}{4}\cos\frac{\theta_\delta+\theta_\alpha}{2} & \sin\frac{(2\theta_\beta+\pi)}{4}\sin\frac{\theta_\delta-\theta_\alpha}{2} \\ -\cos\frac{(2\theta_\beta+\pi)}{4}\sin\frac{\theta_\delta-\theta_\alpha}{2} & \sin\frac{(2\theta_\beta+\pi)}{4}\cos\frac{\theta_\delta+\theta_\alpha}{2} & -\sin\frac{(2\theta_\beta+\pi)}{4}\sin\frac{\theta_\delta+\theta_\alpha}{2} & \cos\frac{(2\theta_\beta+\pi)}{4}\cos\frac{\theta_\delta-\theta_\alpha}{2} \end{pmatrix},$$

$$\tag{74}$$

where θ_α, θ_β, and θ_δ are given by

$$\cos\theta_\alpha \equiv \sqrt{1-\alpha^2}, \quad \sin\theta_\alpha \equiv \alpha, \quad \cos\theta_\beta \equiv \sqrt{1-\beta^2}, \quad \sin\theta_\beta \equiv -\beta,$$

$$\cos\theta_\delta \equiv \frac{\Delta_Z\sqrt{1-\beta^2}}{\Delta_0}\sqrt{1-\alpha^2}, \quad \sin\theta_\delta \equiv \frac{\Delta_{\mathrm{SAS}}}{\Delta_0}\alpha, \tag{75}$$

and

$$\bar{\boldsymbol{n}}_1^g = (1,0,0,0)^t, \quad \bar{\boldsymbol{n}}_2^g = (0,0,1,0)^t. \tag{76}$$

We may introduce perturbative excitation modes η_i by introducing the two CP^3 fields $\boldsymbol{n}_i = U\bar{\boldsymbol{n}}_i$ with

$$\bar{\boldsymbol{n}}_1 = \begin{pmatrix} 1 - \frac{1}{2}|\eta_1|^2 - \frac{1}{2}|\eta_3|^2 \\ \eta_1 \\ -\frac{1}{2}\eta_4^\dagger\eta_1 - \frac{1}{2}\eta_2^\dagger\eta_3 \\ \eta_3 \end{pmatrix}, \quad \bar{\boldsymbol{n}}_2 = \begin{pmatrix} -\frac{1}{2}\eta_1^\dagger\eta_4 - \frac{1}{2}\eta_3^\dagger\eta_2 \\ \eta_4 \\ 1 - \frac{1}{2}|\eta_2|^2 - \frac{1}{2}|\eta_4|^2 \\ \eta_2 \end{pmatrix}, \tag{77}$$

where we parameterize as

$$\eta_i(\boldsymbol{x}) = \frac{\sigma_i(\boldsymbol{x}) + i\vartheta_i(\boldsymbol{x})}{\sqrt{2}}, \tag{78}$$

with $i = 1, 2, 3, 4$, obeying the equal-time commutation relations between η_i and η_j, or

$$\left[\eta_i(\boldsymbol{x}, t), \eta_j^\dagger(\boldsymbol{x}, t)\right] = \frac{2}{\rho_0}\delta_{ij}\delta(\boldsymbol{x} - \boldsymbol{y}), \tag{79}$$

or

$$[\sigma_i(\boldsymbol{x}, t), \vartheta_j(\boldsymbol{x}, t)] = \frac{2i}{\rho_0}\delta_{ij}\delta(\boldsymbol{x} - \boldsymbol{y}). \tag{80}$$

They are required so the SU(4) algebraic relation holds for $\mathcal{S}_a$, $\mathcal{P}_a$, and $\mathcal{S}_{ab}$. For a detailed discussion, see Appendix A.

We calculate the isospin components (73) with the use of $\boldsymbol{n}_i = U\bar{\boldsymbol{n}}_i$, and substitute them into the effective Hamiltonian (17). In this way we obtain the effective Hamiltonian for η_i, which is shown to be the same as the one for the NG modes derived in Ref.[19].
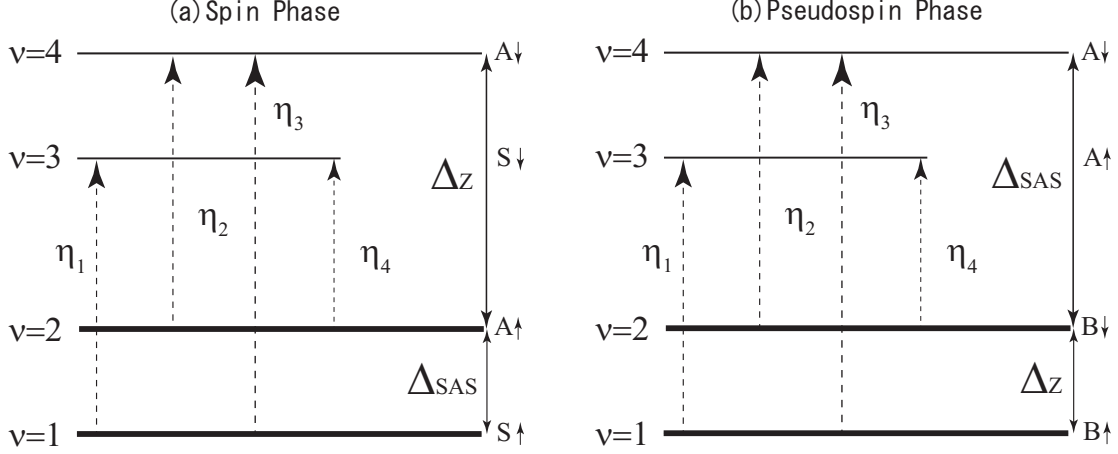
19

FIG. 3: The lowest two energy levels are occupied in the ground state at $\nu = 2$. Small fluctuations are the NG modes η_1, η_2, η_3, and η_4. (a) For the spin phase, η_1 and η_2 describe the fluctuation from the up-spin symmetric state to the down-spin symmetric state and from the up-spin antisymmetric state to the down-spin antisymmetric state, respectively. Their energy levels are degenerated with the Zeeman gap Δ_Z. On the other hand, η_3 and η_4, which are fluctuations from the up-spin symmetric state to the down-spin antisymmetric state and from the up-spin antisymmetric state to the down-spin symmetric state, have an energy gap of $\Delta_Z \pm \Delta_{SAS}$, respectively. (b) For the pseudospin phase η_1 and η_2 describe the fluctuation from the up-spin bonding state to the up-spin antibonding state and from the down-spin bonding state to the down-spin antibonding state, respectively. Their energy levels are degenerated with the tunneling gap Δ_{SAS}. On the other hand, η_3 and η_4, which are fluctuations from the up-spin bonding state to the down-spin antibonding state and from down-spin bonding state to the up-spin antibonding state, have an energy gap of $\Delta_{SAS} \pm \Delta_Z$, respectively.

C. NG modes in the spin phase

As an illustration we study the spin phase at $\sigma_0 = 0$, where the transformation (74) is given by

$$
U = \frac{1}{\sqrt{2}} \begin{pmatrix} 1 & 0 & -1 & 0 \\ 0 & 1 & 0 & -1 \\ 1 & 0 & 1 & 0 \\ 0 & 1 & 0 & 1 \end{pmatrix},
\tag{81}
$$

20

by setting $\alpha, \beta = 0$. We note that

$$\bar{\boldsymbol{n}} = \begin{pmatrix} n^{\mathrm{S}\uparrow} \\ n^{\mathrm{S}\downarrow} \\ n^{\mathrm{A}\uparrow} \\ n^{\mathrm{A}\downarrow} \end{pmatrix} = U^\dagger \begin{pmatrix} n^{\mathrm{f}\uparrow} \\ n^{\mathrm{f}\downarrow} \\ n^{\mathrm{b}\uparrow} \\ n^{\mathrm{b}\downarrow} \end{pmatrix} = U^\dagger \boldsymbol{n}, \tag{82}$$

where

$$n^{\mathrm{S}\alpha} = \frac{1}{\sqrt{2}}(n^{\mathrm{b}\alpha} + n^{\mathrm{f}\alpha}), \quad n^{\mathrm{A}\alpha} = \frac{1}{\sqrt{2}}(n^{\mathrm{b}\alpha} - n^{\mathrm{f}\alpha}), \tag{83}$$

with $\alpha = \uparrow, \downarrow$. The lowest-energy one-body electron state is the up-spin symmetric state, and the second lowest energy state is the up-spin antisymmetric state. They are filled up at $\nu = 2$. The perturbative excitations η_i are as illustrated in Fig. 3 (a).

It follows from (73), (74), and (77) that the isospin densities are explicitly given in terms of $\sigma_i(\boldsymbol{x})$ and $\vartheta_i(\boldsymbol{x})$ by

$$\mathcal{S}_x = \frac{\sigma_1 + \sigma_2}{\sqrt{2}} \equiv \tilde{\sigma}_1, \quad \mathcal{S}_y = \frac{\vartheta_1 + \vartheta_2}{\sqrt{2}} \equiv \tilde{\vartheta}_1, \quad \mathcal{R}_{xx} = \frac{\sigma_1 - \sigma_2}{\sqrt{2}} \equiv \tilde{\sigma}_2, \quad \mathcal{R}_{yx} = \frac{\vartheta_1 - \vartheta_2}{\sqrt{2}} \equiv \tilde{\vartheta}_2,$$

$$\mathcal{R}_{yy} = \frac{\sigma_4 - \sigma_3}{\sqrt{2}} \equiv -\tilde{\sigma}_3, \quad \mathcal{R}_{xy} = \frac{\vartheta_3 - \vartheta_4}{\sqrt{2}} \equiv \tilde{\vartheta}_3, \quad \mathcal{R}_{xz} = -\frac{\sigma_4 + \sigma_3}{\sqrt{2}} \equiv \tilde{\sigma}_4, \quad \mathcal{R}_{yz} = -\frac{\vartheta_4 + \vartheta_3}{\sqrt{2}} \equiv \tilde{\vartheta}_4,$$

$$\mathcal{S}_z = 1 - \sum_{i=1}^{4} \frac{\sigma_i^2 + \vartheta_i^2}{2} = 1 - \sum_{i=1}^{4} \frac{\tilde{\sigma}_i^2 + \tilde{\vartheta}_i^2}{2}, \quad \mathcal{P}_x = \tilde{\sigma}_3 \tilde{\sigma}_4 + \tilde{\vartheta}_3 \tilde{\vartheta}_4, \quad \mathcal{P}_y = \tilde{\sigma}_4 \tilde{\vartheta}_2 - \tilde{\sigma}_2 \tilde{\vartheta}_4,$$

$$\mathcal{P}_z = -\left(\tilde{\sigma}_2 \tilde{\sigma}_3 + \tilde{\vartheta}_2 \tilde{\vartheta}_3\right), \quad \mathcal{R}_{zx} = -\left(\tilde{\sigma}_1 \tilde{\sigma}_2 + \tilde{\vartheta}_1 \tilde{\vartheta}_2\right), \quad \mathcal{R}_{zy} = \tilde{\sigma}_3 \tilde{\vartheta}_1 - \tilde{\sigma}_1 \tilde{\vartheta}_3, \quad \mathcal{R}_{zz} = -\left(\tilde{\sigma}_1 \tilde{\sigma}_4 + \tilde{\vartheta}_1 \tilde{\vartheta}_4\right). \tag{84}$$

Substituting them into (17), we obtain the effective Hamiltonian of the NG modes in terms of the canonical sets of $\tilde{\sigma}_i$ and $\tilde{\vartheta}_i$ as

$$\begin{aligned}
\mathcal{H}^{\mathrm{spin}} = {} & J_s \sum_{a=1,4} \left[(\partial_k \tilde{\sigma}_a)^2 + (\partial_k \tilde{\vartheta}_a)^2\right] + J_s^d \sum_{a=2,3} \left[(\partial_k \tilde{\sigma}_a)^2 + (\partial_k \tilde{\vartheta}_a)^2\right] \\
& + \frac{\rho_0 \Delta_{\mathrm{Z}}}{4} \sum_{=1,4} \left[\tilde{\sigma}_a^2 + \tilde{\vartheta}_a^2\right] + \left(\frac{\rho_0 \Delta_{\mathrm{Z}}}{4} + \rho_0 \epsilon_X^-\right) \sum_{a=2,3} \left[\tilde{\sigma}_a^2 + \tilde{\vartheta}_a^2\right] \\
& - \frac{\rho_0 \Delta_{\mathrm{SAS}}}{2} \left[\tilde{\sigma}_3 \tilde{\sigma}_4 + \tilde{\vartheta}_3 \tilde{\vartheta}_4\right] + \frac{\rho_0 \Delta_{\mathrm{bias}}}{2} \left[\tilde{\sigma}_2 \tilde{\sigma}_3 + \tilde{\vartheta}_2 \tilde{\vartheta}_3\right].
\end{aligned} \tag{85}$$

The annihilation operators are defined by

$$\eta_i^{\mathrm{s}}(\boldsymbol{x}) = \frac{\check{\sigma}_i(\boldsymbol{x}) + i\check{\vartheta}_i(\boldsymbol{x})}{\sqrt{2}}, \tag{86}$$

21

with

$$\check{\sigma}_i \equiv \rho_\Phi^{1/2}\tilde{\sigma}_i, \qquad \check{\vartheta}_i \equiv \rho_\Phi^{1/2}\tilde{\vartheta}_i, \tag{87}$$

and they satisfy the commutation relations

$$\left[\check{\sigma}_i(\boldsymbol{x},t), \check{\vartheta}_j(\boldsymbol{y},t)\right] = i\delta_{ij}\delta(\boldsymbol{x}-\boldsymbol{y}), \tag{88}$$

or

$$\left[\eta_i^{\text{s}}(\boldsymbol{x},t), \eta_j^{\text{s}\dagger}(\boldsymbol{y},t)\right] = \delta_{ij}\delta(\boldsymbol{x}-\boldsymbol{y}), \tag{89}$$

with $i, j = 1, 2, 3, 4$.

The effective Hamiltonian (85) reads in terms of the creation and annihilation variables (86) as

$$\mathcal{H}^{\text{spin}} = \frac{4J_s}{\rho_0}\sum_{a=1,4}\partial_k\eta_a^{\text{s}\dagger}\partial_k\eta_a^{\text{s}} + \frac{4J_s^d}{\rho_0}\sum_{a=2,3}\partial_k\eta_a^{\text{s}\dagger}\partial_k\eta_a^{\text{s}} + \Delta_{\text{Z}}\sum_{a=1,4}\eta_a^{\text{s}\dagger}\eta_a^{\text{s}} + [\Delta_{\text{Z}} + 4\epsilon_X^-]\sum_{a=2,3}\eta_a^{\text{s}\dagger}\eta_a^{\text{s}}$$
$$+ \Delta_{\text{bias}}[\eta_2^{\text{s}\dagger}\eta_3^{\text{s}} + \eta_3^{\text{s}\dagger}\eta_2^{\text{s}}] - \Delta_{\text{SAS}}[\eta_3^{\text{s}\dagger}\eta_4^{\text{s}} + \eta_4^{\text{s}\dagger}\eta_3^{\text{s}}]. \tag{90}$$

The variables η_2^{s}, η_3^{s}, and η_4^{s} are mixing by Δ_{SAS} and Δ_{bias}.

In the momentum space, the annihilation and creation operators are $\eta_{i,\boldsymbol{k}}^{\text{s}}$ and $\eta_{i,\boldsymbol{k}}^{\text{s}\dagger}$ together with the commutation relations

$$\left[\eta_{i,\boldsymbol{k}}^{\text{s}}, \eta_{j,\boldsymbol{k}'}^{\text{s}\dagger}\right] = \delta_{ij}\delta(\boldsymbol{k}-\boldsymbol{k}'). \tag{91}$$

For the sake of the simplicity we consider the balanced configuration with $\Delta_{\text{bias}} = 0$ in the rest of this subsection. Then the Hamiltonian density is given by

$$H^{\text{spin}} = \int d^2k \, \mathcal{H}^{\text{spin}},$$
$$\mathcal{H}^{\text{spin}} = \mathcal{H}_1^{\text{spin}} + \mathcal{H}_2^{\text{spin}} + \mathcal{H}_3^{\text{spin}}, \tag{92}$$

where

$$\mathcal{H}_1^{\text{spin}} = \left[\frac{4J_s}{\rho_0}\boldsymbol{k}^2 + \Delta_{\text{Z}}\right]\eta_{1,\boldsymbol{k}}^{\text{s}\dagger}\eta_{1,\boldsymbol{k}}^{\text{s}}, \tag{93}$$

$$\mathcal{H}_2^{\text{spin}} = \left[\frac{4J_s^d}{\rho_0}\boldsymbol{k}^2 + \Delta_{\text{Z}} + 4\epsilon_X^-\right]\eta_{2,\boldsymbol{k}}^{\text{s}\dagger}\eta_{2,\boldsymbol{k}}^{\text{s}}, \tag{94}$$

$$\mathcal{H}_3^{\text{spin}} = \left[\frac{4J_s^d}{\rho_0}\boldsymbol{k}^2 + \Delta_{\text{Z}} + 4\epsilon_X^-\right]\eta_{3,\boldsymbol{k}}^{\text{s}\dagger}\eta_{3,\boldsymbol{k}}^{\text{s}} + \left[\frac{4J_s}{\rho_0}\boldsymbol{k}^2 + \Delta_{\text{Z}}\right]\eta_{4,\boldsymbol{k}}^{\text{s}\dagger}\eta_{4,\boldsymbol{k}}^{\text{s}} - \Delta_{\text{SAS}}\left[\eta_{3,\boldsymbol{k}}^{\text{s}\dagger}\eta_{4,\boldsymbol{k}}^{\text{s}} + \eta_{4,\boldsymbol{k}}^{\text{s}\dagger}\eta_{3,\boldsymbol{k}}^{\text{s}}\right].$$
$$\tag{95}$$

We first analyze the dispersion relation and the coherence length of $\eta_{1,\boldsymbol{k}}^{\mathrm{s}}$. From (93), we have

$$E_{\eta_1^{\mathrm{s}}}(\boldsymbol{k}) = \frac{4J_s}{\rho_0}\boldsymbol{k}^2 + \Delta_{\mathrm{Z}}, \tag{96}$$

$$\xi_{\eta_1^{\mathrm{s}}} = 2l_B\sqrt{\frac{\pi J_s}{\Delta_{\mathrm{Z}}}}. \tag{97}$$

The coherent length diverges in the limit $\Delta_{\mathrm{Z}} \to 0$. This mode is a pure spin wave since it describes the fluctuation of $\mathcal{S}_x$ and $\mathcal{S}_y$ as in (84). Indeed, the energy (96), as well as the coherent length (97), depend only on the Zeeman gap Δ_{Z} and the intralayer stiffness J_s.

We next analyze those of $\eta_{2,\boldsymbol{k}}^{\mathrm{s}}$:

$$E_{\eta_2^{\mathrm{s}}}(\boldsymbol{k}) = \frac{4J_s^d}{\rho_0}\boldsymbol{k}^2 + \Delta_{\mathrm{Z}} + 4\epsilon_X^-, \tag{98}$$

$$\xi_{\eta_2^{\mathrm{s}}} = 2l_B\sqrt{\frac{\pi J_s^d}{\Delta_{\mathrm{Z}} + 4\epsilon_X^-}}. \tag{99}$$

They depend not only on Δ_{Z} but also on the exchange Coulomb energy ϵ_X^- and the interlayer stiffness originating in the interlayer Coulomb interaction. This mode is a R-spin wave since it describes the fluctuation of $\mathcal{R}_{xx}$ and $\mathcal{R}_{yx}$. From (96) and (98) we see that, in the one body picture, η_1^{s} and η_2^{s} have the same energy gap Δ_{Z}. Indeed, they are described in terms of η_1 and η_2, having the same energy gap Δ_{Z} (Fig. 3 (a)).

We finally analyze those of $\eta_{3,\boldsymbol{k}}^{\mathrm{s}}$ and $\eta_{4,\boldsymbol{k}}^{\mathrm{s}}$, which are coupled. Hamiltonian (95) can be written, in matrix form,

$$\mathcal{H}_3^{\mathrm{spin}} = \begin{pmatrix} \eta_{3,\boldsymbol{k}}^{\mathrm{s}} \\ \eta_{4,\boldsymbol{k}}^{\mathrm{s}} \end{pmatrix}^\dagger \begin{pmatrix} A_{\boldsymbol{k}} & -\Delta_{\mathrm{SAS}} \\ -\Delta_{\mathrm{SAS}} & B_{\boldsymbol{k}} \end{pmatrix} \begin{pmatrix} \eta_{3,\boldsymbol{k}}^{\mathrm{s}} \\ \eta_{4,\boldsymbol{k}}^{\mathrm{s}} \end{pmatrix}, \tag{100}$$

where

$$A_{\boldsymbol{k}} = \frac{4J_s^d}{\rho_0}\boldsymbol{k}^2 + \Delta_{\mathrm{Z}} + 4\epsilon_X^-, \quad B_{\boldsymbol{k}} = \frac{4J_s}{\rho_0}\boldsymbol{k}^2 + \Delta_{\mathrm{Z}}. \tag{101}$$

Hamiltonian (100) can be diagonalized as

$$\mathcal{H}_3^{\mathrm{spin}} = \begin{pmatrix} \tilde{\eta}_{3,\boldsymbol{k}}^{\mathrm{s}} \\ \tilde{\eta}_{4,\boldsymbol{k}}^{\mathrm{s}} \end{pmatrix}^\dagger \begin{pmatrix} E^{\tilde{\eta}_3^{\mathrm{s}}} & 0 \\ 0 & E^{\tilde{\eta}_4^{\mathrm{s}}} \end{pmatrix} \begin{pmatrix} \tilde{\eta}_{3,\boldsymbol{k}}^{\mathrm{s}} \\ \tilde{\eta}_{4,\boldsymbol{k}}^{\mathrm{s}} \end{pmatrix}, \tag{102}$$

where

$$E^{\tilde{\eta}_3^{\mathrm{s}}} = \frac{1}{2}\left[A_{\boldsymbol{k}} + B_{\boldsymbol{k}} + \sqrt{(A_{\boldsymbol{k}} - B_{\boldsymbol{k}})^2 + 4\Delta_{\mathrm{SAS}}^2}\right], \quad E^{\tilde{\eta}_4^{\mathrm{s}}} = \frac{1}{2}\left[A_{\boldsymbol{k}} + B_{\boldsymbol{k}} - \sqrt{(A_{\boldsymbol{k}} - B_{\boldsymbol{k}})^2 + 4\Delta_{\mathrm{SAS}}^2}\right],$$

$$\tag{103}$$

and the annihilation operator $\tilde{\eta}^{\text{s}}_{i,\boldsymbol{k}}$ ($i = 3, 4$) given by the form

$$\tilde{\eta}^{\text{s}}_{3,\boldsymbol{k}} = \frac{\left(\sqrt{C_{\boldsymbol{k}}^2 + 4\Delta_{\text{SAS}}^2} + C_{\boldsymbol{k}}\right)\eta_{3,\boldsymbol{k}} - 2\Delta_{\text{SAS}}\eta_{4,\boldsymbol{k}}}{\sqrt{2\left(C_{\boldsymbol{k}}^2 + 4\Delta_{\text{SAS}}^2 + C_{\boldsymbol{k}}\sqrt{C_{\boldsymbol{k}}^2 + 4\Delta_{\text{SAS}}^2}\right)}},$$

$$\tilde{\eta}^{\text{s}}_{4,\boldsymbol{k}} = \frac{\left(\sqrt{C_{\boldsymbol{k}}^2 + 4\Delta_{\text{SAS}}^2} - C_{\boldsymbol{k}}\right)\eta_{3,\boldsymbol{k}} + 2\Delta_{\text{SAS}}\eta_{4,\boldsymbol{k}}}{\sqrt{2\left(C_{\boldsymbol{k}}^2 + 4\Delta_{\text{SAS}}^2 - C_{\boldsymbol{k}}\sqrt{C_{\boldsymbol{k}}^2 + 4\Delta_{\text{SAS}}^2}\right)}}, \tag{104}$$

with $C_{\boldsymbol{k}} = A_{\boldsymbol{k}} - B_{\boldsymbol{k}}$. The annihilation operators (104) satisfy the commutation relations

$$\left[\tilde{\eta}^{\text{s}}_{i,\boldsymbol{k}}, \tilde{\eta}^{\text{s}\dagger}_{j,\boldsymbol{k}'}\right] = \delta_{ij}\delta(\boldsymbol{k} - \boldsymbol{k}'), \tag{105}$$

with $i, j = 3, 4$. We obtain the dispersions for the modes $\tilde{\eta}^{\text{s}}_{i,\boldsymbol{k}}$ ($i = 3, 4$) from (101) and (103).

By taking the limit $\boldsymbol{k} \to 0$ in (103), we have two gaps

$$E^{\tilde{\eta}^{\text{s}}_3}_{\boldsymbol{k}=0} = \Delta_{\text{Z}} + 2\epsilon_X^- + \left[4(\epsilon_X^-)^2 + \Delta_{\text{SAS}}^2\right]^{\frac{1}{2}}, \quad E^{\tilde{\eta}^{\text{s}}_4}_{\boldsymbol{k}=0} = \Delta_{\text{Z}} + 2\epsilon_X^- - \left[4(\epsilon_X^-)^2 + \Delta_{\text{SAS}}^2\right]^{\frac{1}{2}}. \tag{106}$$

The gapless condition ($E^{\tilde{\eta}^{\text{s}}_4}_{\boldsymbol{k}=0} = 0$) implies

$$\Delta_{\text{Z}}(\Delta_{\text{Z}} + 4\epsilon_X^-) - \Delta_{\text{SAS}}^2 = 0, \tag{107}$$

which holds only along the boundary of the spin and CAF phases: see (4.17) in Ref.[22]. In the interior of the spin phase we have $\Delta_{\text{Z}}(\Delta_{\text{Z}} + 4\epsilon_X^-) - \Delta_{\text{SAS}}^2 > 0$, which implies that no gapless modes arise from $\tilde{\eta}^{\text{s}}_3$ and $\tilde{\eta}^{\text{s}}_4$. From (106), in the one body picture, $\tilde{\eta}^{\text{s}}_3$ and $\tilde{\eta}^{\text{s}}_4$ have the energy gap $\Delta_{\text{Z}} \pm \Delta_{\text{SAS}}$, respectively. Indeed they are described in terms of η_3 and η_4 (Fig. 3 (a)). These excitation modes are R-spin waves coupled with the layer degree of freedom. There emerge four complex NG modes, one describing the spin wave (η^{s}_1), and the other three the R-spin waves ($\eta^{\text{s}}_2, \eta^{\text{s}}_3, \eta^{\text{s}}_4$).

D. NG modes in the pseudospin phase

For the pseudospin phase, β is identified with the imbalanced parameter σ_0, as we discussed in Sect. IV A with (64). In this subsection, instead of β we express the effective Hamiltonian, the dispersions, and the coherence length in terms of σ_0, since it is a physical variable.

From (74), by setting $\alpha = 1$, we have

$$U = \frac{1}{\sqrt{2}} \begin{pmatrix} \sqrt{1+\sigma_0} & -\sqrt{1-\sigma_0} & 0 & 0 \\ 0 & 0 & -\sqrt{1+\sigma_0} & -\sqrt{1-\sigma_0} \\ \sqrt{1-\sigma_0} & \sqrt{1+\sigma_0} & 0 & 0 \\ 0 & 0 & -\sqrt{1-\sigma_0} & \sqrt{1+\sigma_0} \end{pmatrix}, \tag{108}$$

and

$$\bar{\boldsymbol{n}} = \begin{pmatrix} n^{\mathrm{B}\uparrow} \\ n^{\mathrm{A}\uparrow} \\ -n^{\mathrm{B}\downarrow} \\ n^{\mathrm{A}\downarrow} \end{pmatrix} = U^\dagger \begin{pmatrix} n^{\mathrm{f}\uparrow} \\ n^{\mathrm{f}\downarrow} \\ n^{\mathrm{b}\uparrow} \\ n^{\mathrm{b}\downarrow} \end{pmatrix} = U^\dagger \boldsymbol{n}, \tag{109}$$

where

$$n^{\mathrm{B}\alpha} = \frac{1}{\sqrt{2}}(\sqrt{1-\sigma_0}\, n^{\mathrm{b}\alpha} + \sqrt{1+\sigma_0}\, n^{\mathrm{f}\alpha}), \quad n^{\mathrm{A}\alpha} = \frac{1}{\sqrt{2}}(\sqrt{1+\sigma_0}\, n^{\mathrm{b}\alpha} - \sqrt{1-\sigma_0}\, n^{\mathrm{f}\alpha}), \tag{110}$$

with $\alpha = \uparrow, \downarrow$. The lowest-energy one-body electron state is the up-spin bonding state, and the second lowest energy state is the down-spin bonding state. They are filled up at $\nu = 2$. The perturbative excitations η_i are as illustrated in Fig. 3 (b).

We go on to derive the effective Hamiltonian governing these NG modes. From (73), (74), and (77), the isospin densities are given in terms of $\tilde{\sigma}_i(\boldsymbol{x})$ and $\tilde{\vartheta}_i(\boldsymbol{x})$ as:

$$\mathcal{P}_x = \sigma_0 \tilde{\sigma}_2 + \sqrt{1-\sigma_0^2}\left(1 - \sum_{i=1}^{4} \frac{\tilde{\sigma}_i^2 + \tilde{\vartheta}_i^2}{2}\right), \qquad \mathcal{P}_z = -\sqrt{1-\sigma_0^2}\,\tilde{\sigma}_2 + \sigma_0\left(1 - \sum_{i=1}^{4} \frac{\tilde{\sigma}_i^2 + \tilde{\vartheta}_i^2}{2}\right),$$

$$\mathcal{S}_x = -\left(\tilde{\sigma}_1\tilde{\sigma}_4 + \tilde{\vartheta}_1\tilde{\vartheta}_4\right), \quad \mathcal{S}_y = \tilde{\sigma}_1\tilde{\vartheta}_3 - \tilde{\sigma}_3\tilde{\vartheta}_1, \quad \mathcal{S}_z = \tilde{\sigma}_3\tilde{\sigma}_4 + \tilde{\vartheta}_3\tilde{\vartheta}_4,$$

$$\mathcal{R}_{zy} = \tilde{\vartheta}_1, \qquad \mathcal{P}_y = \tilde{\vartheta}_2, \qquad \mathcal{R}_{xy} = \tilde{\vartheta}_3, \qquad \mathcal{R}_{yy} = \tilde{\sigma}_4,$$

$$\mathcal{R}_{xx} = -\sqrt{1-\sigma_0^2}\left(\tilde{\sigma}_2\tilde{\sigma}_3 + \tilde{\vartheta}_2\tilde{\vartheta}_3\right) + \sigma_0\tilde{\sigma}_3, \quad \mathcal{R}_{xz} = -\sigma_0\left(\tilde{\sigma}_2\tilde{\sigma}_3 + \tilde{\vartheta}_2\tilde{\vartheta}_3\right) - \sqrt{1-\sigma_0^2}\,\tilde{\sigma}_3,$$

$$\mathcal{R}_{yx} = \sqrt{1-\sigma_0^2}\left(\tilde{\sigma}_2\tilde{\vartheta}_4 - \tilde{\sigma}_4\tilde{\vartheta}_2\right) - \sigma_0\tilde{\vartheta}_4, \quad \mathcal{R}_{yz} = \sigma_0\left(\tilde{\sigma}_2\tilde{\vartheta}_4 - \tilde{\sigma}_4\tilde{\vartheta}_2\right) + \sqrt{1-\sigma_0^2}\,\tilde{\vartheta}_4,$$

$$\mathcal{R}_{zx} = -\sqrt{1-\sigma_0^2}\left(\tilde{\sigma}_1\tilde{\sigma}_2 + \tilde{\vartheta}_1\tilde{\vartheta}_2\right) + \sigma_0\tilde{\sigma}_1, \quad \mathcal{R}_{zz} = -\sigma_0\left(\tilde{\sigma}_1\tilde{\sigma}_2 + \tilde{\vartheta}_1\tilde{\vartheta}_2\right) - \sqrt{1-\sigma_0^2}\,\tilde{\sigma}_1 \tag{111}$$

Now, we substitute the isospin densities (111) into the effective Hamiltonian (17). In this way we derive the effective Hamiltonian of the NG modes in terms of the canonical sets of $\tilde{\sigma}_i$ and $\tilde{\vartheta}_i$ (or with $\check{\sigma}_i$ and $\check{\vartheta}_i$).

25

In the momentum space, this reads

$$\int d^2 k \mathcal{H}^{\mathrm{p}} = \int d^2 k \mathcal{H}_1^{\mathrm{p}} + \int d^2 k \mathcal{H}_2^{\mathrm{p}} + \int d^2 k \mathcal{H}_3^{\mathrm{p}}, \tag{112}$$

where

$$\mathcal{H}_1^{\mathrm{p}} = A_{\boldsymbol{k}}^{\mathrm{p}} \check{\sigma}_{1,\boldsymbol{k}}^{\dagger} \check{\sigma}_{1,\boldsymbol{k}} + B_{\boldsymbol{k}}^{\mathrm{p}} \check{\vartheta}_{1,\boldsymbol{k}}^{\dagger} \check{\vartheta}_{1,\boldsymbol{k}}, \tag{113}$$

$$\mathcal{H}_2^{\mathrm{p}} = C_{\boldsymbol{k}}^{\mathrm{p}} \check{\sigma}_{2,\boldsymbol{k}}^{\dagger} \check{\sigma}_{2,\boldsymbol{k}} + B_{\boldsymbol{k}}^{\mathrm{p}} \check{\vartheta}_{2,\boldsymbol{k}}^{\dagger} \check{\vartheta}_{2,\boldsymbol{k}}, \tag{114}$$

$$\mathcal{H}_3^{\mathrm{p}} = (\vec{P}_{\boldsymbol{k}}^{\mathrm{p}})^{\dagger} \mathcal{M}^{\mathrm{p}} \vec{P}_{\boldsymbol{k}}^{\mathrm{p}}, \tag{115}$$

with $\check{\sigma}_{i,\boldsymbol{k}}$, and $\check{\vartheta}_{i,\boldsymbol{k}}$ given by (87), and

$$A_{\boldsymbol{k}}^{\mathrm{p}} = \frac{2J_1^{\sigma_0}}{\rho_0} k^2 + \frac{\Delta_{\mathrm{SAS}}}{2\sqrt{1-\sigma_0^2}} - 2\epsilon_X^-(1-\sigma_0^2), \quad B_{\boldsymbol{k}}^{\mathrm{p}} = \frac{2J_s^d}{\rho_0} k^2 + \frac{\Delta_{\mathrm{SAS}}}{2\sqrt{1-\sigma_0^2}},$$

$$C_{\boldsymbol{k}}^{\mathrm{p}} = \frac{2J_1^{\sigma_0}}{\rho_0} k^2 + \frac{\Delta_{\mathrm{SAS}}}{2\sqrt{1-\sigma_0^2}} + \epsilon_{\mathrm{cap}}(1-\sigma_0^2), \quad J_1^{\sigma_0} = (1-\sigma_0^2)J_s + \sigma_0^2 J_s^d,$$

$$\vec{P}_{\boldsymbol{k}}^{\mathrm{p}} = \begin{pmatrix} \check{\vartheta}_4 \\ \check{\vartheta}_3 \\ \check{\sigma}_3 \\ \check{\sigma}_4 \end{pmatrix}, \quad \mathcal{M}^{\mathrm{p}} = \begin{pmatrix} A_{\boldsymbol{k}}^{\mathrm{p}} & -\Delta_{\mathrm{Z}}/2 & 0 & 0 \\ -\Delta_{\mathrm{Z}}/2 & B_{\boldsymbol{k}}^{\mathrm{p}} & 0 & 0 \\ 0 & 0 & A_{\boldsymbol{k}}^{\mathrm{p}} & -\Delta_{\mathrm{Z}}/2 \\ 0 & 0 & -\Delta_{\mathrm{Z}}/2 & B_{\boldsymbol{k}}^{\mathrm{p}} \end{pmatrix}. \tag{116}$$

We first analyze the dispersions and the coherence lengths from (114), since it describes the pseudospin wave. It is diagonalized as:

$$H_2^{\mathrm{p}} = \int d^2 k E_2^{\mathrm{p}} \eta_{2,\boldsymbol{k}}^{\mathrm{p}\dagger} \eta_{2,\boldsymbol{k}}^{\mathrm{p}} \tag{117}$$

with

$$E_{2,\boldsymbol{k}}^{\mathrm{p}} = 2\sqrt{B_{\boldsymbol{k}}^{\mathrm{p}} C_{\boldsymbol{k}}^{\mathrm{p}}}, \tag{118}$$

$$\eta_{2,\boldsymbol{k}}^{\mathrm{p}} = \frac{1}{\sqrt{2}} \left(\left(\frac{C_{\boldsymbol{k}}^{\mathrm{p}}}{B_{\boldsymbol{k}}^{\mathrm{p}}}\right)^{\frac{1}{4}} \check{\sigma}_{2,\boldsymbol{k}} + i \left(\frac{B_{\boldsymbol{k}}^{\mathrm{p}}}{C_{\boldsymbol{k}}^{\mathrm{p}}}\right)^{\frac{1}{4}} \check{\vartheta}_{2,\boldsymbol{k}} \right), \tag{119}$$

where $\eta_{2,\boldsymbol{k}}^{\mathrm{p}}$ satisfy the commutation relation

$$\left[\eta_{2,\boldsymbol{k}}^{\mathrm{p}}, \eta_{2,\boldsymbol{k}'}^{\mathrm{p}\dagger} \right] = \delta(\boldsymbol{k} - \boldsymbol{k}'). \tag{120}$$

Since the ground state is a squeezed coherent state due to the capacitance energy ϵ_{cap}, it is more convenient[3] to use the dispersion and the coherence lengths of $\check{\sigma}_2$ and $\check{\vartheta}_2$ separately. The dispersion relations are given by

$$E_{\boldsymbol{k}}^{\check{\sigma}_2} = \frac{2J_1^{\sigma_0}}{\rho_0} \boldsymbol{k}^2 + \frac{\Delta_{\mathrm{SAS}}}{2\sqrt{1-\sigma_0^2}} + \epsilon_{\mathrm{cap}}(1-\sigma_0^2), \quad E_{\boldsymbol{k}}^{\check{\vartheta}_2} = \frac{2J_s^d}{\rho_0} \boldsymbol{k}^2 + \frac{\Delta_{\mathrm{SAS}}}{2\sqrt{1-\sigma_0^2}}, \tag{121}$$

26

and their coherence lengths are

$$\xi^{\check{\sigma}_2} = 2l_B \sqrt{\frac{\pi J_1^{\sigma_0}}{\frac{\Delta_{\text{SAS}}}{\sqrt{1-\sigma_0^2}} + 2\epsilon_{\text{cap}}(1-\sigma_0^2)}}, \quad \xi^{\check{\vartheta}_2} = 2l_B \sqrt{\frac{\pi J_s^d \sqrt{1-\sigma_0^2}}{\Delta_{\text{SAS}}}}. \tag{122}$$

A similar analysis can be adopted for (113), which is diagonalized as:

$$H_1^{\text{p}} = \int d^2 k E_1^{\text{p}} \eta_{1,\mathbf{k}}^{\text{p}\dagger} \eta_{1,\mathbf{k}}^{\text{p}} \tag{123}$$

with

$$E_1^{\text{p}} = 2\sqrt{B_{\mathbf{k}}^{\text{p}} A_{\mathbf{k}}^{\text{p}}}, \tag{124}$$

$$\eta_{1,\mathbf{k}}^{\text{p}} = \frac{1}{\sqrt{2}} \left(\left(\frac{A_{\mathbf{k}}^{\text{p}}}{B_{\mathbf{k}}^{\text{p}}} \right)^{\frac{1}{4}} \check{\sigma}_{1,\mathbf{k}} + i \left(\frac{B_{\mathbf{k}}^{\text{p}}}{A_{\mathbf{k}}^{\text{p}}} \right)^{\frac{1}{4}} \check{\vartheta}_{1,\mathbf{k}} \right), \tag{125}$$

where $\eta_{1,\mathbf{k}}^{\text{p}}$ satisfy the commutation relation

$$\left[\eta_{1,\mathbf{k}}^{\text{p}}, \eta_{1,\mathbf{k}'}^{\text{p}\dagger} \right] = \delta(\mathbf{k} - \mathbf{k}'). \tag{126}$$

The dispersion relations of the canonical sets of $\check{\sigma}_1$ and $\check{\vartheta}_1$ are given by

$$E_{\mathbf{k}}^{\check{\sigma}_1} = \frac{2J_1^{\sigma_0}}{\rho_0} \mathbf{k}^2 + \frac{\Delta_{\text{SAS}}}{2\sqrt{1-\sigma_0^2}} - 2\epsilon_X^-(1-\sigma_0^2), \quad E_{\mathbf{k}}^{\check{\vartheta}_1} = \frac{2J_s^d}{\rho_0} \mathbf{k}^2 + \frac{\Delta_{\text{SAS}}}{2\sqrt{1-\sigma_0^2}}. \tag{127}$$

Their coherence lengths are

$$\xi^{\check{\sigma}_1} = 2l_B \sqrt{\frac{\pi J_1^{\sigma_0}}{\frac{\Delta_{\text{SAS}}}{\sqrt{1-\sigma_0^2}} - 4\epsilon_X^-(1-\sigma_0^2)}}, \quad \xi^{\check{\vartheta}_1} = 2l_B \sqrt{\frac{\pi J_s^d \sqrt{1-\sigma_0^2}}{\Delta_{\text{SAS}}}}. \tag{128}$$

It appears that $\xi^{\check{\sigma}_1}$ is ill-defined for $\Delta_{\text{SAS}} \to 0$ in (128). This is not the case due to the relation (130) in the pseudospin phase, which we mention soon. We see that from (118) and (124), in the one body picture, η_1^{p} and η_2^{p} have the same energy gap Δ_{SAS}. They are described in terms of η_1 and η_2, having the same energy gap Δ_{SAS} (Fig. 3 (b)).

Finally, analyzing of the Hamiltonian (115) as in the case of the spin phase, we obtain the condition for the existence of a gapless mode:

$$\frac{\Delta_{\text{SAS}}}{\sqrt{1-\sigma_0^2}} \left[\frac{\Delta_{\text{SAS}}}{\sqrt{1-\sigma_0^2}} - 4\epsilon_X^-(1-\sigma_0^2) \right] - \Delta_Z^2 = 0. \tag{129}$$

This occurs along the pseudospin-canted boundary: see (5.3) and (5.4) in Ref. [22]. Inside the pseudospin phase, since we have

$$\frac{\Delta_{\text{SAS}}}{\sqrt{1-\sigma_0^2}} \left[\frac{\Delta_{\text{SAS}}}{\sqrt{1-\sigma_0^2}} - 4\epsilon_X^-(1-\sigma_0^2) \right] - \Delta_Z^2 > 0, \tag{130}$$

there are no gapless modes.

E. NG modes in the CAF phase

We derive the effective Hamiltonian of the NG modes in terms of the canonical sets of $\check{\sigma}_i$ and $\check{\vartheta}_i$. This can be done by substituting (A8) and (A9) into the Hamiltonian (17). We first derive the Hamiltonian, without taking any limits. Since the expression becomes too extensive, we introduce the notation

$$c_{\theta_\alpha} \equiv \cos\theta_\alpha, \quad s_{\theta_\alpha} \equiv \sin\theta_\alpha, \quad c_{\theta_\beta} \equiv \cos\theta_\beta, \quad s_{\theta_\beta} \equiv \sin\theta_\beta, \quad c_{\theta_\delta} \equiv \cos\theta_\delta, \quad s_{\theta_\delta} \equiv \sin\theta_\delta. \tag{131}$$

to make the expression for the effective Hamiltonian more manageable.

Working in the momentum space, the effective Hamiltonian reads

$$H^{\mathrm{c}} = \int d^2 k \mathcal{H}^{\mathrm{c}} = \int d^2 k \mathcal{H}^{\mathrm{c}}_1 + \int d^2 k \mathcal{H}^{\mathrm{c}}_2, \tag{132}$$

where

$$\mathcal{H}^{\mathrm{c}}_1 = \left(\frac{2}{\rho_0} J_1^\alpha \boldsymbol{k}^2 + \frac{\Delta_0 c_{\theta_\beta}^{-1}}{2}\right) \check{\vartheta}^\dagger_{1,\boldsymbol{k}} \check{\vartheta}_{1,\boldsymbol{k}} + \left(\frac{2}{\rho_0}(c_{\theta_\delta}^2 J_s + s_{\theta_\delta}^2 J_1^\beta)\boldsymbol{k}^2 + \frac{M - 4(s_{\theta_\delta}^2 c_{\theta_\beta}^2 + c_{\theta_\delta}^2)\epsilon_X^-}{2}\right) \check{\sigma}^\dagger_{1,\boldsymbol{k}} \check{\sigma}_{1,\boldsymbol{k}}, \tag{133}$$

$$\mathcal{H}^{\mathrm{c}}_2 = \vec{Q}^{\mathrm{c}\dagger}_{\boldsymbol{k}} \mathcal{M}^{\mathrm{c}}_2 \vec{Q}^{\mathrm{c}}_{\boldsymbol{k}}, \tag{134}$$

with

$$J_1^\alpha = c_{\theta_\alpha}^2 J_s + s_{\theta_\alpha}^2 J_s^d, \quad M = 4c_{\theta_\alpha}^2 \epsilon_X^- + \Delta_0 c_{\theta_\beta}^{-1},$$

$$\vec{Q}^{\mathrm{c}}_{\boldsymbol{k}} = \begin{pmatrix} \check{\vartheta}_{2,\boldsymbol{k}} \\ \check{\vartheta}_{4,\boldsymbol{k}} \\ \check{\vartheta}_{3,\boldsymbol{k}} \\ \check{\sigma}_{2,\boldsymbol{k}} \\ \check{\sigma}_{4,\boldsymbol{k}} \\ \check{\sigma}_{3,\boldsymbol{k}} \end{pmatrix}, \quad \mathcal{M}^{\mathrm{c}}_2 = \begin{pmatrix} A^{\mathrm{c}} & c^{\mathrm{c}} & -e^{\mathrm{c}} & 0 & 0 & 0 \\ c^{\mathrm{c}} & C^{\mathrm{c}} & -f^{\mathrm{c}} & 0 & 0 & 0 \\ -e^{\mathrm{c}} & -f^{\mathrm{c}} & F^{\mathrm{c}} & 0 & 0 & 0 \\ 0 & 0 & 0 & B^{\mathrm{c}} & a^{\mathrm{c}} & b^{\mathrm{c}} \\ 0 & 0 & 0 & a^{\mathrm{c}} & D^{\mathrm{c}} & d^{\mathrm{c}} \\ 0 & 0 & 0 & b^{\mathrm{c}} & d^{\mathrm{c}} & E^{\mathrm{c}} \end{pmatrix}. \tag{135}$$

The Matrix elements in (135) are given by

$$A^{\mathrm{c}} = \frac{2\boldsymbol{k}^2}{\rho_0}\left[c_{\theta_\delta}^2 J_3^\beta + s_{\theta_\delta}^2 J_s^d\right] + \frac{M}{2} - 2s_{\theta_\beta}^2 c_{\theta_\delta}^2 \epsilon_X^-, \quad B^{\mathrm{c}} = \frac{2\boldsymbol{k}^2}{\rho_0}\left[c_{\theta_\alpha}^2 J_3^\beta + s_{\theta_\alpha}^2 J_1^\beta\right] + \frac{\Delta_0}{2c_{\theta_\beta}} + \frac{c_{\theta_\beta}^2 \epsilon_\alpha}{2},$$

$$C^{\mathrm{c}} = \frac{2\boldsymbol{k}^2}{\rho_0}J_1^\beta + \frac{M}{2} - 2c_{\theta_\beta}^2 \epsilon_X^-, \quad D^{\mathrm{c}} = \frac{2\boldsymbol{k}^2}{\rho_0}\left[c_{\theta_\delta}^2\left(s_{\theta_\alpha}^2 J_3^\beta + c_{\theta_\alpha}^2 J_1^\beta\right) + s_{\theta_\delta}^2 J_1^\alpha\right] + \frac{\Delta_0}{2c_{\theta_\beta}} + \frac{c_{\theta_\delta}^2 s_{\theta_\beta}^2 \epsilon_\alpha}{2},$$

$$E^{\mathrm{c}} = \frac{2\boldsymbol{k}^2}{\rho_0}\left[s_{\theta_\delta}^2\left(c_{\theta_\alpha}^2 J_3^\beta + s_{\theta_\alpha}^2 J_1^\beta\right) + c_{\theta_\delta}^2 J_3^\alpha\right] + \frac{M}{2} + s_{\theta_\beta}^2 s_{\theta_\delta}^2 c_{\theta_\alpha}^2 \epsilon_{\mathrm{cap}} - 2(c_{\theta_\beta}^2 s_{\theta_\delta}^2 + c_{\theta_\delta}^2)s_{\theta_\alpha}^2 \epsilon_X^-,$$

$$F^{\mathrm{c}} = \frac{2\boldsymbol{k}^2}{\rho_0}J_s^d + \frac{M}{2}, \tag{136}$$

and

$$a^{\mathrm{c}} = \frac{2\boldsymbol{k}^2}{\rho_0}c_{\theta_\delta}c_{2\theta_\alpha}J_2^\beta + \frac{s_{2\theta_\beta}c_{\theta_\delta}}{4}\epsilon_\alpha, \quad b^{\mathrm{c}} = -\frac{2\boldsymbol{k}^2}{\rho_0}s_{\theta_\delta}s_{2\theta_\alpha}J_2^\beta + L + \frac{\Delta_{\mathrm{SAS}}}{4\Delta_0}c_{\theta_\alpha}s_{2\theta_\beta}\epsilon_\alpha,$$

$$c^{\mathrm{c}} = \frac{2\boldsymbol{k}^2}{\rho_0}c_{\theta_\delta}J_2^\beta + s_{2\theta_\beta}c_{\theta_\delta}\epsilon_X^-,$$

$$d^{\mathrm{c}} = -\frac{s_{2\theta_\alpha}s_{2\theta_\delta}}{4}\left[\frac{2\boldsymbol{k}^2}{\rho_0}\left(J_1^\beta + J_s^d - J_3^\beta - J_s\right) + s_{\theta_\beta}^2(2\epsilon_X^- - \epsilon_{\mathrm{cap}})\right] - \frac{N}{2},$$

$$e^{\mathrm{c}} = -\frac{L}{2}, \quad f^{\mathrm{c}} = \frac{N}{2}, \tag{137}$$

with

$$J_3^\alpha = c_{\theta_\alpha}^2 J_s^d + s_{\theta_\alpha}^2 J_s, \quad J_1^\beta = c_{\theta_\beta}^2 J_s + s_{\theta_\beta}^2 J_s^d, \quad J_2^\beta = \frac{s_{2\theta_\beta}}{2}(J_s^d - J_s), \quad J_3^\beta = c_{\theta_\beta}^2 J_s^d + s_{\theta_\beta}^2 J_s,$$

$$L = -\frac{s_{2\theta_\beta}}{2}\left[s_{\theta_\delta}s_{2\theta_\alpha}(2\epsilon_X^- - \epsilon_{\mathrm{cap}}) + c_{\theta_\alpha}\frac{\Delta_{\mathrm{SAS}}}{\Delta_0}\epsilon_\alpha\right], \quad \epsilon_\alpha = 4c_{\theta_\alpha}^2 \epsilon_X^- + 2s_{\theta_\alpha}^2 \epsilon_{\mathrm{cap}},$$

$$N = \frac{s_{2\theta_\delta}s_{2\theta_\alpha}s_{\theta_\beta}^2}{2}(2\epsilon_X^- - \epsilon_{\mathrm{cap}}) + \frac{\Delta_{\mathrm{SAS}}}{\Delta_0}(c_{\theta_\delta}c_{\theta_\alpha}s_{\theta_\beta}^2 \epsilon_\alpha + \Delta_Z), \tag{138}$$

where we denote $s_{2\theta_\alpha} = \sin 2\theta_\alpha$, $s_{2\theta_\beta} = \sin 2\theta_\beta$, and $s_{2\theta_\delta} = \sin 2\theta_\delta$.

It can be verified that the effective Hamiltonian (133) and (134) reproduces the effective Hamiltonian in the spin phase (92) by taking the limit $\alpha, \beta \to 0$. On the other hand, we reproduce the effective Hamiltonian in the pseudospin phase (112) by taking the limit $\alpha \to 1$ in (133) and (134).

The effective Hamiltonian in the CAF phase is too complicated to make a further analysis. We take the limit $\Delta_{\mathrm{SAS}} \to 0$ to examine if some simplified formulas are obtained. In particular we would like to seek gapless modes. Such gapless modes will play an important role in driving the interlayer coherence in the CAF phase. In this limit, we have:

$$\cos\theta_\beta = \frac{\Delta_{\mathrm{SAS}}}{\Delta_{\mathrm{Z}}}, \quad \sin\theta_\beta = \pm\sqrt{1 - \left(\frac{\Delta_{\mathrm{SAS}}}{\Delta_{\mathrm{Z}}}\right)^2}, \quad \cos\theta_\delta = \cos\theta_\alpha, \quad \sin\theta_\delta = \sin\theta_\alpha,$$

$$\alpha^2 = |\sigma_0|. \tag{139}$$

From (58) and (139), the classical ground state reads:

$$\mathcal{S}_z^0 = 1 - |\sigma_0|, \quad \mathcal{P}_z^0 = \sigma_0, \quad \mathcal{R}_{xx}^0 = \mathrm{sgn}(\sigma_0)\mathcal{R}_{yy}^0, \quad \mathcal{R}_{yy}^0 = -\sqrt{|\sigma_0|(1 - |\sigma_0|)}, \tag{140}$$

all others being zero. We assume $\sigma_0 > 0$ for definiteness. The transformation (74) has a simple expression:

$$U^\dagger = \begin{pmatrix} 1 & 0 & 0 & 0 \\ 0 & \sqrt{1 - |\sigma_0|} & \sqrt{|\sigma_0|} & 0 \\ 0 & -\sqrt{|\sigma_0|} & \sqrt{1 - |\sigma_0|} & 0 \\ 0 & 0 & 0 & 1 \end{pmatrix}, \tag{141}$$

We find $\bar{\boldsymbol{n}} = U^\dagger \boldsymbol{n}$ is of the form $(n^{\mathrm{f}\uparrow}, n_{\mathrm{f}\downarrow\mathrm{b}\uparrow}^{\mathrm{S}}, n_{\mathrm{f}\downarrow\mathrm{b}\uparrow}^{\mathrm{A}}, n^{\mathrm{b}\downarrow})^t$ by setting

$$n_{\mathrm{f}\downarrow\mathrm{b}\uparrow}^{\mathrm{S}} = (\sqrt{1 - |\sigma_0|}n^{\mathrm{f}\downarrow} + \sqrt{|\sigma_0|}n^{\mathrm{b}\uparrow}), \quad n_{\mathrm{f}\downarrow\mathrm{b}\uparrow}^{\mathrm{A}} = (-\sqrt{|\sigma_0|}n^{\mathrm{f}\downarrow} + \sqrt{1 - |\sigma_0|}n^{\mathrm{b}\uparrow}). \tag{142}$$

Consequently, the ground state is such that $|n^{\mathrm{f}\uparrow}\rangle$ and $|n_{\mathrm{f}\downarrow\mathrm{b}\uparrow}^{\mathrm{A}}\rangle$ are filled up: The NG modes η_1 and η_3 describe an excitation from the state $|n^{\mathrm{f}\uparrow}\rangle$ to $|n_{\mathrm{f}\downarrow\mathrm{b}\uparrow}^{\mathrm{S}}\rangle$ and $|n^{\mathrm{b}\downarrow}\rangle$, respectively, while the NG modes η_2 and η_4 describe an excitation from the state $|n_{\mathrm{f}\downarrow\mathrm{b}\uparrow}^{\mathrm{A}}\rangle$ to $|n^{\mathrm{b}\downarrow}\rangle$ and $|n_{\mathrm{f}\downarrow\mathrm{b}\uparrow}^{\mathrm{S}}\rangle$, respectively. A similar analysis can be done for $\sigma_0 < 0$: $|n^{\mathrm{b}\uparrow}\rangle$ and $|n_{\mathrm{f}\uparrow\mathrm{b}\downarrow}^{\mathrm{S}}\rangle$ are filled up, where

$$n_{\mathrm{f}\uparrow\mathrm{b}\downarrow}^{\mathrm{S}} = (\sqrt{1 - |\sigma_0|}n^{\mathrm{f}\uparrow} + \sqrt{|\sigma_0|}n^{\mathrm{b}\downarrow}), \quad n_{\mathrm{f}\downarrow\mathrm{b}\uparrow}^{\mathrm{A}} = (-\sqrt{|\sigma_0|}n^{\mathrm{f}\uparrow} + \sqrt{1 - |\sigma_0|}n^{\mathrm{b}\downarrow}), \tag{143}$$

and the gapless mode η_4 describes an excitation from the state $|n_{\mathrm{f}\uparrow\mathrm{b}\downarrow}^{\mathrm{S}}\rangle$ to $|n_{\mathrm{f}\uparrow\mathrm{b}\downarrow}^{\mathrm{A}}\rangle$.

By using (139) with (133), and (134) with (135), (136), (137), and (138), we have the Hamiltonian

$$H = \sum_{i=1}^{4} \int d^2 k E_i \eta_{i,\boldsymbol{k}}^{\mathrm{c}\dagger} \eta_{i,\boldsymbol{k}}^{\mathrm{c}}, \tag{144}$$

together with the dispersion relations (Fig. 4):

$$E_1 = E_2 = \frac{4\boldsymbol{k}^2}{\rho_0}J_1^\alpha + \Delta_{\mathrm{Z}}, \quad E_3 = \frac{4\boldsymbol{k}^2}{\rho_0}J_s^d + 2\Delta_{\mathrm{Z}} + 8\cos^2\theta_\alpha \epsilon_X^-,$$

$$E_4 = |\boldsymbol{k}|\sqrt{\frac{8J_s^d}{\rho_0}\left(\frac{2\boldsymbol{k}^2}{\rho_0}(\cos^2 2\theta_\alpha J_s^d + \sin^2 2\theta_\alpha J_s) + 2\sin^2 2\theta_\alpha(\epsilon_D^- - \epsilon_X^-)\right)}, \tag{145}$$

where $\eta_{i,\boldsymbol{k}}^{\mathrm{c}}$ ($i = 1, 2, 3, 4$) are the annihilation operators

$$\eta_{1,\boldsymbol{k}}^{\mathrm{c}} = \frac{\check{\vartheta}_{1,\boldsymbol{k}} - i\check{\sigma}_{1,\boldsymbol{k}}}{\sqrt{2}}, \quad \eta_{2,\boldsymbol{k}}^{\mathrm{c}} = \frac{\check{\vartheta}_{2,\boldsymbol{k}} - i\check{\sigma}_{2,\boldsymbol{k}}}{\sqrt{2}}, \quad \eta_{3,\boldsymbol{k}}^{\mathrm{c}} = \left(\frac{\rho_0}{4}\right)^{\frac{1}{2}}(\sigma_{3,\boldsymbol{k}} + i\vartheta_{3,\boldsymbol{k}}),$$

$$\eta_{4,\boldsymbol{k}}^{\mathrm{c}} = \left(\frac{\rho_0}{4}\right)^{\frac{1}{2}}\left(\left(\frac{\lambda^{\sigma_4}}{\lambda^{\vartheta_4}}\right)^{\frac{1}{4}}\sigma_{4,\boldsymbol{k}} + i\left(\frac{\lambda^{\vartheta_4}}{\lambda^{\sigma_4}}\right)^{\frac{1}{4}}\vartheta_{4,\boldsymbol{k}}\right), \tag{146}$$
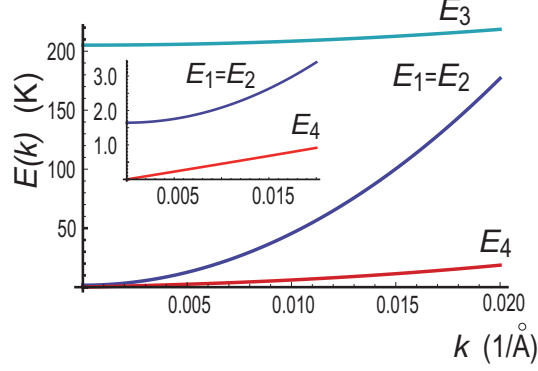
FIG. 4: Dispersion relations (145) for the four NG modes E_i. The sample parameters are $d = 231$, $B \approx 5.6$T, $\rho_0 = 2.7 \times 10^{15}$m^{-2}, and $\alpha = 0.1$. Inset: Dispersion relations near $k = 0$. It is clear that $E_4(k)$ is linear.

with

$$\lambda^{\vartheta_4} = \frac{2\boldsymbol{k}^2}{\rho_0} J_s^d, \quad \lambda^{\sigma_4} = \frac{2\boldsymbol{k}^2}{\rho_0}(\cos^2 2\theta_\alpha J_s^d + \sin^2 2\theta_\alpha J_s) + 2\sin^2 2\theta_\alpha(\epsilon_D^- - \epsilon_X^-). \tag{147}$$

The annihilation operators $\eta_{i,\boldsymbol{k}}$ satisfy the commutation relation,

$$\left[\eta_{i,\boldsymbol{k}}^{\mathrm{c}}, \eta_{j,\boldsymbol{k}'}^{\mathrm{c}\dagger}\right] = \delta_{ij}\delta(\boldsymbol{k} - \boldsymbol{k}'), \tag{148}$$

with $i, j = 1, 2, 3, 4$.

We summarize the NG modes in the CAF phase in the limit $\Delta_{\mathrm{SAS}} \to 0$. It is to be emphasized that there emerges one gapless mode, $\eta_{4,\boldsymbol{k}}^{\mathrm{c}}$, reflecting the realization of the exact and its spontaneous breaking of the U(1) symmetry generated by $\frac{T_{yx}-T_{xy}}{\sqrt{2}}$. Furthermore, it has the linear dispersion relation as in (145), which leads to a superfluidity associated with this gapless mode. All other modes have gaps.

F. CAF phase in $\Delta_{\mathrm{SAS}} \to 0$ up to $\mathcal{O}(\Delta_{\mathrm{SAS}}^3)$

We focus solely on the gapless mode η_4^{c} (or η_4) by neglecting all other gapped modes, and derive the effective Hamiltonian for η_4 up to $\mathcal{O}(\Delta_{\mathrm{SAS}}^3)$. We assume $\sigma_0 > 0$ for simplicity.

The two CP^3 fields to be used in the perturbation theory are given by $\bar{\boldsymbol{n}} = U^\dagger \boldsymbol{n}$ with (74) and

31

(77), or

$$\bar{\boldsymbol{n}}_1 = \begin{pmatrix} 1 \\ 0 \\ 0 \\ 0 \end{pmatrix}, \quad \bar{\boldsymbol{n}}_2 = \begin{pmatrix} 0 \\ \eta_4 \\ 1 - \frac{1}{2}|\eta_4|^2 \\ 0 \end{pmatrix}, \tag{149}$$

Using (62), we can exactly determine β as

$$\beta^2 = \frac{\Delta_{\text{SAS}}^2 \alpha^2 + \Delta_{\text{Z}}^2(1 - \alpha^2)}{\Delta_{\text{SAS}}^2 \alpha^4 + \sigma_0^2 \Delta_{\text{Z}}^2(1 - \alpha^2)} \sigma_0^2. \tag{150}$$

Note that in the limit $\Delta_{\text{SAS}} \to 0$ we obtain $\beta \to 1$, which is in accord with our previous calculations. Substituting (150) into (59), we find

$$\Delta_{\text{Z}}^2 = \frac{\Delta_{\text{SAS}}^2 \alpha^4 + \sigma_0^2 \Delta_{\text{Z}}^2(1 - \alpha^2)}{\alpha^2(\alpha^2 - \sigma_0^2)} + 4\epsilon_X^- \frac{\sigma_0^2 - \alpha^4}{\alpha^3} \frac{\sqrt{\Delta_{\text{SAS}}^2 \alpha^2 + \Delta_{\text{Z}}^2(1 - \alpha^2)}}{\sqrt{\alpha^2 - \sigma_0^2}}. \tag{151}$$

The relation (151) determines the value of α^2 as a function of Δ_{Z}, Δ_{SAS}, and σ_0. Substituting this value into (150) we obtain β^2 as a function of Δ_{Z}, Δ_{SAS}, σ_0. We have thus summarized our problem into a single equation (151). When Δ_{SAS} is exactly zero, (151) yields the relation $\alpha^2 = |\sigma_0|$. Therefore, for weak tunnelings, we search for a solution in the form

$$\alpha^2 = |\sigma_0| + \lambda \Delta_{\text{SAS}}^2 + \mathcal{O}(\Delta_{\text{SAS}}^4), \tag{152}$$

where we expect λ to be a constant. In order to find the value of λ we use (152) and expand the relevant combinations in powers of Δ_{SAS}^2. In particular, for the first and second terms of (151) we find

$$\frac{\Delta_{\text{SAS}}^2 \alpha^4 + \sigma_0^2 \Delta_{\text{Z}}^2(1 - \alpha^2)}{\alpha^2(\alpha^2 - \sigma_0^2)} = \Delta_{\text{Z}}^2 \left[1 + \frac{(1 - \lambda \Delta_{\text{Z}}^2)\Delta_{\text{SAS}}^2}{(1 - |\sigma_0|)\Delta_{\text{Z}}^2} - \frac{\lambda(2 - |\sigma_0|)}{|\sigma_0|(1 - |\sigma_0|)}\Delta_{\text{SAS}}^2 \right] + \mathcal{O}(\Delta_{\text{SAS}}^4),$$

$$4\epsilon_X^- \frac{\sigma_0^2 - \alpha^4}{\alpha^3} \frac{\sqrt{\Delta_{\text{SAS}}^2 \alpha^2 + \Delta_{\text{Z}}^2(1 - \alpha^2)}}{\sqrt{\alpha^2 - \sigma_0^2}} = -\lambda \frac{8\epsilon_X^- \Delta_{\text{Z}}}{|\sigma_0|}\Delta_{\text{SAS}}^2 + \mathcal{O}(\Delta_{\text{SAS}}^4). \tag{153}$$

Substituting these into (151) we obtain

$$\Delta_{\text{Z}}^2 = \Delta_{\text{Z}}^2 \left[1 + \frac{(1 - \lambda \Delta_{\text{Z}}^2)\Delta_{\text{SAS}}^2}{(1 - |\sigma_0|)\Delta_{\text{Z}}^2} - \frac{\lambda(2 - |\sigma_0|)}{|\sigma_0|(1 - |\sigma_0|)}\Delta_{\text{SAS}}^2 \right] - \lambda \frac{8\epsilon_X^- \Delta_{\text{Z}}}{|\sigma_0|}\Delta_{\text{SAS}}^2 + \mathcal{O}(\Delta_{\text{SAS}}^4). \tag{154}$$

The lowest terms Δ_{SAS}^0 disappear automatically. Requiring the Δ_{SAS}^2-terms to vanish, we obtain

$$\lambda = \frac{1}{\Delta_{\text{Z}}} \frac{|\sigma_0|}{2(\Delta_{\text{Z}} + 4\epsilon_X^-(1 - |\sigma_0|))}, \tag{155}$$

32

and for α^2 we summarize as

$$\alpha^2 = |\sigma_0| \left(1 + \frac{\Delta_Z}{2(\Delta_Z + 4\epsilon_X^-(1 - |\sigma_0|))} \frac{\Delta_{SAS}^2}{\Delta_Z^2} \right) + \mathcal{O}(\Delta_{SAS}^4). \tag{156}$$

Using this in (150) we come to

$$\beta^2 = 1 - \frac{\Delta_{SAS}^2}{\Delta_Z^2} + \mathcal{O}(\Delta_{SAS}^4). \tag{157}$$

Finally, using (156) and (157) in (75) and (60), we find:

$$\sin^2 \theta_\delta = |\sigma_0| \left(1 + \frac{\Delta_Z + 8\epsilon_X^-(1 - |\sigma_0|))}{2(\Delta_Z + 4\epsilon_X^-(1 - |\sigma_0|))} \frac{\Delta_{SAS}^2}{\Delta_Z^2} \right) + \mathcal{O}(\Delta_{SAS}^4) \tag{158}$$

$$\Delta_{bias} = \text{sgn}(\sigma_0)\Delta_Z \left[1 + \frac{4\epsilon_X^- + 8(\epsilon_D^- - \epsilon_X^-)|\sigma_0|}{\Delta_Z} - \frac{1}{2}\frac{\Delta_{SAS}^2}{\Delta_Z^2} \right] + \mathcal{O}(\Delta_{SAS}^4), \tag{159}$$

respectively. Then by using (156), (157), (158), and (159) with (17), we obtain the effective Hamiltonian for the gapless mode η_4 (σ_4 and ϑ_4):

$$\mathcal{H} = \frac{J_{\vartheta_4}}{2}(\nabla\vartheta_4)^2 + \frac{J_{\sigma_4}}{2}(\nabla\sigma_4)^2 + 4\rho_0(\epsilon_D^- - \epsilon_X^-)|\sigma_0| \left(1 - |\sigma_0| - \frac{1}{2}\frac{\Delta_{SAS}^2}{\Delta_Z^2} \right), \tag{160}$$

with

$$J_{\vartheta_4} = 2\left(J_s^d + J_s^- \frac{\Delta_{SAS}^2}{\Delta_Z^2} \right), \quad J_{\sigma_4} = 2\left(J_s^d + 8J_s^-|\sigma_0|(1 - |\sigma_0|) + J_s^-(1 - 4|\sigma_0|)\frac{\Delta_{SAS}^2}{\Delta_Z^2} \right). \tag{161}$$

Taking $\Delta_{SAS}^2 = 0$, we reproduce the previously calculated expressions (144) and (145).

We wish to derive the effective Hamiltonian for the nonperturbative analysis of the phase field $\vartheta(\boldsymbol{x})$. For this purpose, it is necessary to start with the parameterization of the Grassmannian field valid for arbitrary values of $\vartheta(\boldsymbol{x})$. We make an ansatz

$$\boldsymbol{n}_2 = \begin{pmatrix} 0 \\ -e^{+i\vartheta(\boldsymbol{x})}\sqrt{\sigma(\boldsymbol{x})} \\ \sqrt{1 - \sigma(\boldsymbol{x})} \\ 0 \end{pmatrix} = e^{i\sigma_0\vartheta(\boldsymbol{x})} \begin{pmatrix} 0 \\ -e^{+i(1-\sigma_0)\vartheta(\boldsymbol{x})}\sqrt{\sigma(\boldsymbol{x})} \\ e^{-i\sigma_0\vartheta(\boldsymbol{x})}\sqrt{1 - \sigma(\boldsymbol{x})} \\ 0 \end{pmatrix}. \tag{162}$$

We expand it around $\vartheta(\boldsymbol{x}) = 0$ and $\sigma(\boldsymbol{x}) = \sigma_0$ by setting $\delta\sigma(\boldsymbol{x}) \equiv \sigma(\boldsymbol{x}) - \sigma_0$. Up to the linear orders in $\vartheta(\boldsymbol{x})$ and $\delta\sigma(\boldsymbol{x})$, it is straightforward to show that

$$e^{+i(1-\sigma_0)\vartheta(\boldsymbol{x})}\sqrt{\sigma(\boldsymbol{x})} = \sqrt{\sigma_0} - \sqrt{1 - \sigma_0}\eta_4(\boldsymbol{x}),$$

$$e^{-i\sigma_0\vartheta(\boldsymbol{x})}\sqrt{1 - \sigma(\boldsymbol{x})} = \sqrt{1 - \sigma_0} + \sqrt{\sigma_0}\eta_4(\boldsymbol{x}), \tag{163}$$

33

where we have set

$$\eta_4(\boldsymbol{x}) = -\frac{\sigma(\boldsymbol{x}) - \sigma_0}{2\sqrt{\sigma_0(1 - \sigma_0)}} - i\vartheta(\boldsymbol{x})\sqrt{\sigma_0(1 - \sigma_0)}. \tag{164}$$

By requiring the commutation relation (79), we find

$$\frac{\rho_0}{2}[\sigma(\boldsymbol{x}), \vartheta(\boldsymbol{y})] = i\delta(\boldsymbol{x} - \boldsymbol{y}) \tag{165}$$

We have shown that the CP^3 field (162) is reduced to $\boldsymbol{n}_2$ in (149) in the linear order of the perturbation fields, apart from the U(1) factor $e^{-i\sigma_0\vartheta(\boldsymbol{x})}$. We may drop it off the parameterization since the CP^3 field is defined up to such a U(1) factor. Indeed, such a factor does not contribute to the isospin fields.

Here we parameterize the CP^3 fields as

$$\boldsymbol{n}_1 = \begin{pmatrix} 1 \\ 0 \\ 0 \\ 0 \end{pmatrix}, \quad \boldsymbol{n}_2 = \begin{pmatrix} 0 \\ -e^{+i\vartheta(\boldsymbol{x})/2}\sqrt{\sigma(\boldsymbol{x})} \\ e^{-i\vartheta(\boldsymbol{x})/2}\sqrt{1 - \sigma(\boldsymbol{x})} \\ 0 \end{pmatrix}, \tag{166}$$

for $\sigma(\boldsymbol{x}) > 0$, and

$$\boldsymbol{n}_1 = \begin{pmatrix} 0 \\ 0 \\ 1 \\ 0 \end{pmatrix}, \quad \boldsymbol{n}_2 = \begin{pmatrix} e^{+i\vartheta(\boldsymbol{x})/2}\sqrt{1 + \sigma(\boldsymbol{x})} \\ 0 \\ 0 \\ e^{-i\vartheta(\boldsymbol{x})/2}\sqrt{-\sigma(\boldsymbol{x})} \end{pmatrix}. \tag{167}$$

for $\sigma(\boldsymbol{x}) < 0$. The isospin density fields are expressed in terms of $\sigma(\boldsymbol{x})$ and $\vartheta(\boldsymbol{x})$:

$$\mathcal{S}_z(\boldsymbol{x}) = 1 - |\sigma(\boldsymbol{x})|, \quad \mathcal{P}_z(\boldsymbol{x}) = \sigma(\boldsymbol{x}),$$

$$\mathcal{R}_{yy}(\boldsymbol{x}) = \text{sgn}(\sigma_0)\mathcal{R}_{xx}(\boldsymbol{x}) = -\sqrt{|\sigma(\boldsymbol{x})|(1 - |\sigma(\boldsymbol{x})|)}\cos\vartheta(\boldsymbol{x}),$$

$$\mathcal{R}_{yx}(\boldsymbol{x}) = -\text{sgn}(\sigma_0)\mathcal{R}_{xy}(\boldsymbol{x}) = -\sqrt{|\sigma(\boldsymbol{x})|(1 - |\sigma(\boldsymbol{x})|)}\sin\vartheta(\boldsymbol{x}), \tag{168}$$

with all others being zero. The ground-state expectation values are $\langle\sigma(\boldsymbol{x})\rangle = \sigma_0$, $\langle\vartheta(\boldsymbol{x})\rangle = 0$, with which the order parameters (140) are reproduced from (168). It is notable that the fluctuations of the phase field $\vartheta(\boldsymbol{x})$ affect both the spin and pseudospin components of the R-spin. This is very different from the spin wave in the monolayer QH system or the pseudospin wave in the bilayer QH system at $\nu = 1$. Hence we call it the entangled spin-pseudospin phase field $\vartheta(\boldsymbol{x})$.

By substituting (168) into (17), apart from irrelevant constant terms, the resulting effective Hamiltonian is:

$$\mathcal{H}_{\text{eff}} = \frac{J_\vartheta}{2}(\nabla\vartheta)^2 + \frac{J_\sigma}{2}(\nabla\sigma)^2 + \rho_\Phi\epsilon_{\text{cap}}^{\nu=1}(\sigma - \sigma_0)^2, \tag{169}$$

where we have used

$$\Delta_{\text{bias}} = \text{sgn}(\sigma_0) \left[\Delta_Z + 4\epsilon_X^- + 2\epsilon_{\text{cap}}^{\nu=1} |\sigma_0| \right], \tag{170}$$

$$J_\sigma = 4J_s + \frac{(2|\sigma_0| - 1)^2}{|\sigma_0|(1 - |\sigma_0|)} J_s^d, \quad J_\vartheta = 4J_s^d |\sigma_0|(1 - |\sigma_0|). \tag{171}$$

When we require the equal-time commutation relation,

$$\frac{\rho_0}{2} \left[\sigma(\boldsymbol{x}), \vartheta(\boldsymbol{y}) \right] = i\delta(\boldsymbol{x} - \boldsymbol{y}), \tag{172}$$

the Hamiltonian (169) is second quantized, and it has the linear dispersion relation

$$E_{\boldsymbol{k}} = |\boldsymbol{k}| \sqrt{\frac{2J_\vartheta}{\rho_0} \left(\frac{2J_\sigma}{\rho_0} \boldsymbol{k}^2 + 2\epsilon_{\text{cap}}^{\nu=1} \right)}. \tag{173}$$

This agrees with E_4 in Eq. (145). It should be emphasized that the effective Hamiltonian (169) is valid in all orders of the phase field $\vartheta(\boldsymbol{x})$. It may be regarded as a classical Hamiltonian as well, where (172) should be replaced with the corresponding Poisson bracket.

The effective Hamiltonian (169) for $\vartheta(\boldsymbol{x})$ and $\sigma(\boldsymbol{x})$ reminds us of the one that governs the Josephson effect at $\nu = 1$. The main difference is the absence of the tunneling term, which implies that there exists no Josephson tunneling. We have shown that the effective Hamiltonian is correct up to $\mathcal{O}(\Delta_{\text{SAS}}^3)$ as $\Delta_{\text{SAS}} \to 0$. Nevertheless, the Josephson supercurrent is present within the layer, which is our main issue.

By using the Hamiltonian (169) and the commutation relation (172), we obtain the equations of motion:

$$\hbar \partial_t \vartheta(\boldsymbol{x}) = \frac{2J_\sigma}{\rho_0} \nabla^2 \sigma(\boldsymbol{x}) - 2\epsilon_{\text{cap}}^{\nu=1} (\sigma(\boldsymbol{x}) - \sigma_0), \tag{174}$$

$$\hbar \partial_t \sigma(\boldsymbol{x}) = -\frac{2J_\vartheta}{\rho_0} \nabla^2 \vartheta(\boldsymbol{x}). \tag{175}$$

G. Josephson supercurrents in the CAF phase

We now study the electric Josephson supercurrent carried by the gapless mode $\vartheta(\boldsymbol{x})$ in the CAF phase, where the further analysis goes in parallel with that given for $\nu = 1$.

The electron densities are $\rho_e^{\text{f(b)}} = -e\rho_0 \left(1 \pm \mathcal{P}_z \right)/2 = -e\rho_0 \left(1 \pm \sigma(\boldsymbol{x}) \right)/2$ on each layer. Taking the time derivative and using (175), we find

$$\partial_t \rho_e^{\text{f}} = -\partial_t \rho_e^{\text{b}} = \frac{eJ_\vartheta}{\hbar} \nabla^2 \vartheta(\boldsymbol{x}). \tag{176}$$

35

The time derivative of the charge is associated with the current via the continuity equation, $\partial_t \rho_e^{\mathrm{f(b)}} = \partial_i \mathcal{J}_i^{\mathrm{f(b)}}$. We thus identify $\mathcal{J}_i^{\mathrm{f(b)}} = \pm \mathcal{J}_i^{\mathrm{Jos}}(\boldsymbol{x}) + \mathrm{constant}$, where

$$\mathcal{J}_i^{\mathrm{Jos}}(\boldsymbol{x}) \equiv \frac{e J_\vartheta}{\hbar} \partial_i \vartheta(\boldsymbol{x}). \tag{177}$$

Consequently, the current $\mathcal{J}_x^{\mathrm{Jos}}(\boldsymbol{x})$ flows when there exists inhomogeneity in the phase $\vartheta(\boldsymbol{x})$. Such a current is precisely the Josephson supercurrent. It is intriguing that the current does not flow in the balanced system since $J_\vartheta = 0$ at $\sigma_0 = 0$.

H. Quantum Hall effects in the CAF phase

Let us inject the current $\mathcal{J}_{\mathrm{in}}$ into the x direction of the bilayer sample, and assume the system to be homogeneous in the y direction (Fig. 5). By applying the same argument as given in Sect. III E, we show the anomalous Hall resistance behaviours affected by the phase coherence in the CAF phase.

The current for each layer is the sum of the Hall current and the Josephson current,

$$\mathcal{J}_x^{\mathrm{f}}(x) = \frac{\nu}{R_{\mathrm{K}}} \frac{\rho_0^{\mathrm{f}}}{\rho_0} E_y + \mathcal{J}_x^{\mathrm{Jos}}, \quad \mathcal{J}_x^{\mathrm{b}}(x) = \frac{\nu}{R_{\mathrm{K}}} \frac{\rho_0^{\mathrm{b}}}{\rho_0} E_y - \mathcal{J}_x^{\mathrm{Jos}}. \tag{178}$$

We apply these formulas to analyze the counterflow and drag experiments without tunneling. With the same argument as given in Sect. III E, we have

$$R_{xy}^{\mathrm{f}} \equiv \frac{E_y^{\mathrm{f}}}{\mathcal{J}_x^{\mathrm{f}}} = 0, \qquad R_{xy}^{\mathrm{b}} \equiv \frac{E_y^{\mathrm{b}}}{\mathcal{J}_x^{\mathrm{b}}} = 0 \tag{179}$$

in the counterflow experiment. All the input current is carried by the Josephson supercurrent, $\mathcal{J}_x^{\mathrm{Jos}} = \mathcal{J}_{\mathrm{in}}$. It generates such an inhomogeneous phase field that $\vartheta(\boldsymbol{x}) = (\hbar/e J_\vartheta)\mathcal{J}_{\mathrm{in}} x$.

On the other hand, in the drag experiment, we have $\mathcal{J}_{\mathrm{in}} = \mathcal{J}_x^{\mathrm{f}} = (\nu/R_{\mathrm{K}})E_y$, or

$$R_{xy}^{\mathrm{f}} \equiv \frac{E_y^{\mathrm{f}}}{\mathcal{J}_x^{\mathrm{f}}} = \frac{R_{\mathrm{K}}}{\nu} = \frac{1}{2} R_{\mathrm{K}} \qquad \text{at} \quad \nu = 2. \tag{180}$$

A part of the input current is carried by the Josephson supercurrent, $\mathcal{J}_x^{\mathrm{Jos}} = \frac{1}{2}(1 - \sigma_0)\mathcal{J}_{\mathrm{in}}$.

In conclusion, we predict the anomalous Hall resistance (179) and (180) in the CAF phase at $\nu = 2$ by carrying out similar experiments[8–10] due to Kellogg et al. and Tutuc et al. in the imbalanced configuration ($\sigma_0 \neq 0$).
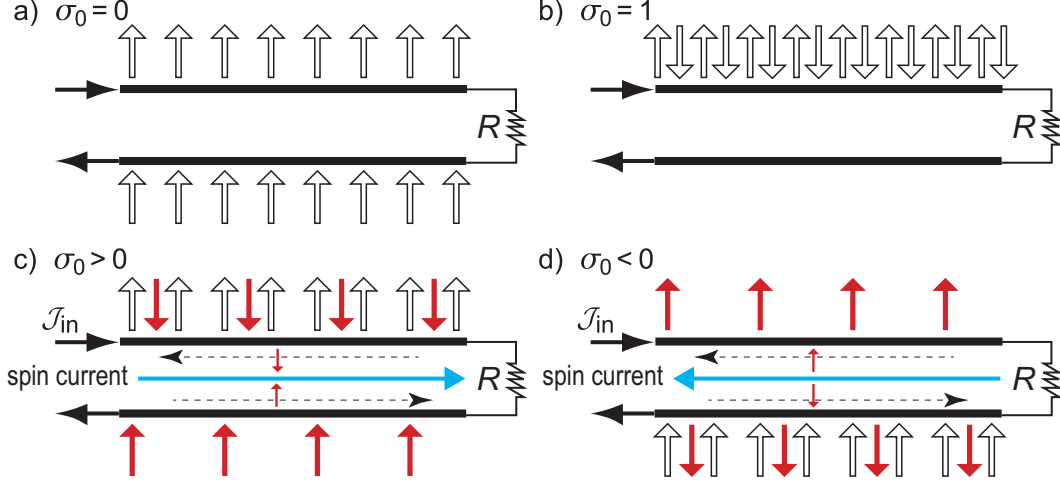
FIG. 5: Schematic illustration of the spin supercurrent flowing along the x-axis in the counterflow geometry. (a) All spins are polarized into the positive z axis due to the Zeeman effect at $\sigma_0 = 0$. No spin current flows. (b) All electrons belong to the front layer at $\sigma_0 = 1$. No spin current flows. (c) In the CAF phase for $\sigma_0 > 0$, some up-spin electrons are moved from the back layer to the front layer by flipping spins. An NG mode appears associated with this charge-spin transfer. The interlayer phase difference $\vartheta(\boldsymbol{x})$ is created by feeding a charge current $\mathscr{J}_{\text{in}}$ to the front layer, which also drives the spin current. Electrons flow in each layer as indicated by the dotted horizontal arrows, and the spin current flows as indicated by the solid horizontal arrow. (d) In the CAF phase for $\sigma_0 < 0$, similar phenomena occur but the direction of the spin current becomes opposite.

I. Spin Josephson supercurrent in the CAF phase

An intriguing feature of the CAF phase is that the phase field $\vartheta(\boldsymbol{x})$ describes the entangled spin-pseudospin coherence according to the basic formula (168).

Up to $\mathcal{O}((\sigma - \sigma_0)^2)$, we have $\mathcal{S}_z = 1 - |\sigma(\boldsymbol{x})|$, and we obtain

$$\partial_t \rho_{\text{b}\uparrow}^{\text{spin}} = \partial_t \rho_{\text{f}\downarrow}^{\text{spin}} = \frac{J_\vartheta}{4}[1 + \text{sgn}(\sigma_0)]\partial_x^2 \vartheta(\boldsymbol{x}), \tag{181}$$

$$\partial_t \rho_{\text{f}\uparrow}^{\text{spin}} = \partial_t \rho_{\text{b}\downarrow}^{\text{spin}} = -\frac{J_\vartheta}{4}[1 - \text{sgn}(\sigma_0)]\partial_x^2 \vartheta(\boldsymbol{x}). \tag{182}$$

The time derivative of the spin is associated with the spin current via the continuity equation,

$\partial_t \rho_\alpha^{\mathrm{spin}}(\boldsymbol{x}) = \partial_x \mathcal{J}_\alpha^{\mathrm{spin}}(\boldsymbol{x})$ for each α. We thus identify

$$\mathcal{J}_{\mathrm{b\uparrow}}^{\mathrm{spin}}(\boldsymbol{x}) = \mathcal{J}_{\mathrm{f\downarrow}}^{\mathrm{spin}}(\boldsymbol{x}) = \frac{J_\vartheta}{2} \partial_x \vartheta(\boldsymbol{x}), \quad \text{for } \sigma_0 > 0, \tag{183}$$

$$\mathcal{J}_{\mathrm{f\uparrow}}^{\mathrm{spin}}(\boldsymbol{x}) = \mathcal{J}_{\mathrm{b\downarrow}}^{\mathrm{spin}}(\boldsymbol{x}) = -\frac{J_\vartheta}{2} \partial_x \vartheta(\boldsymbol{x}), \quad \text{for } \sigma_0 < 0. \tag{184}$$

The spin current $\mathcal{J}_\alpha^{\mathrm{spin}}(\boldsymbol{x})$ flows along the x axis, when there exists an inhomogeneous phase difference $\vartheta(\boldsymbol{x})$.

In the counterflow experiment, the total charge current along the x axis is zero: $\mathcal{J}_x^{\mathrm{f}}(\boldsymbol{x}) + \mathcal{J}_x^{\mathrm{b}}(\boldsymbol{x}) = 0$. Consequently, the input current generates a pure spin current along the x-axis,

$$\mathcal{J}_x^{\mathrm{spin}} = \mathcal{J}_{\mathrm{f\uparrow}}^{\mathrm{spin}} + \mathcal{J}_{\mathrm{f\downarrow}}^{\mathrm{spin}} + \mathcal{J}_{\mathrm{b\uparrow}}^{\mathrm{spin}} + \mathcal{J}_{\mathrm{b\downarrow}}^{\mathrm{spin}} = \mathrm{sgn}(\sigma_0) \frac{\hbar}{e} \mathcal{J}_{\mathrm{in}}. \tag{185}$$

This current is dissipationless since the dispersion relation is linear. It is appropriate to call it a spin Josephson supercurrent. It is intriguing that the spin current flows in the opposite directions for $\sigma_0 > 0$ and $\sigma_0 < 0$, as illustrated in Fig.5. A comment is in order: The spin current only flows within the sample, since spins are scattered in the resistor R and spin directions become random outside the sample.

V. CONCLUSION

In this paper, we have derived the effective Hamiltonian for the NG modes based on the Grassmannian formalism. We have first reproduced the perturbative results on the dispersions and coherence lengths obtained in Ref.[19]. We have then presented the effective theory describing the interlayer coherence in the bilayer QH system at $\nu = 1, 2$. The Grassmannian formalism shows a clear physical picture of the spontaneous development of an interlayer phase coherence. It is to be emphasized that the Grassmannian formalism enables us to analyze nonperturbative phase coherent phenomena such as the Josephson supercurrent. The nonperturbative analysis was beyond the scope of Ref.[19]. It has been argued[3] that the interlayer coherence is due to the Bose-Einstein condensation of composite bosons, which are single electrons bound to magnetic flux quanta. The composite bosons are described by the CP fields, from which the Grassmannian field is composed.

We have explored the phase-coherent phenomena in the bilayer system. At $\nu = 1$, the interlayer phase coherence due to the pseudospin, governed by the NG mode describing a pseudospin wave, is developed spontaneously. On the other hand, the phase coherence in the CAF phase is the

entangled spin-pseudospin phase coherence governed by the NG mode $\vartheta(\boldsymbol{x})$ describing the R-spin according to the formula (168). We have predicted the anomalous Hall resistivity in the counterflow and drag experiments. It has been shown to exhibit precisely the same behaviour for $\nu = 1$ and $\nu = 2$. The difference between them is that the supercurrent flows both in balanced and imbalanced systems at $\nu = 1$ but only in imbalanced systems at $\nu = 2$. Furthermore, a spin Josephson supercurrent flows in the CAF phase in the counterflow geometry, but not for $\nu = 1$. In other words, the net spin current is nonzero for the CAF phase, while it is zero for $\nu = 1$. This is due to the spin structure such that the spins are canted coherently and making antiferromagnetic correlations between the two layers at $\nu = 2$, while the spin is actually frozen and therefore all of the spins are pointing to the positive z axis in both layers at $\nu = 1$ in the limit $\Delta_{\text{SAS}} \to 0$.

Acknowledgment

[1] K. v. Klitzing, G. Dorda, and M. Pepper, Phys. Rev. Lett. **45**, 494 (1980).

[2] D. C. Tsui, H. L. Stormer, and A. C. Gossard, Phys. Rev. Lett. **48**, 1559 (1982).

[3] Z. F. Ezawa, *Quantum Hall effects: Field theoretical approach and related topics, Second Edition* (World Scientific, Singapore, 2008).

[4] *Perspectives in Quantum Hall Effects,* edited by S. Das Sarma and A. Pinczuk (Wiley, New york, 1997).

[5] Z. F. Ezawa and A. Iwazaki, Int. J. Mod. Phys. B **6**, 3205 (1992); Phys. Rev. B **47**, 7295 (1993); Phys. Rev. B **48**, 15189 (1993).

[6] X. G. Wen and A. Zee, Phys. Rev. Lett. **69**, 1811 (1992); Phys. Rev. B **47**, 2265 (1993).

[7] I. B. Spielman, J. P. Eisenstein, L. N. Pfeiffer, and K. W. West, Phys. Rev. Lett. **84**, 5808 (2000).

[8] M. Kellogg, J. P. Eisenstein, L. N. Pfeiffer, and K. W. West, Phys. Rev. Lett. **93**, 036801 (2004).

[9] E. Tutuc, M. Shayegan, and D. A. Huse, Phys. Rev. Lett. **93**, 036802 (2004).

[10] M. Kellogg, I. B. Spielman, J. P. Eisenstein, L. N. Pfeiffer, and K. W. West, Phys. Rev. Lett. **88**, 126804 (2002).

[11] L. Tiemann, W. Dietsche, M. Hauser, and K. von Klitzing, New. J. Phys. **10**, 045018 (2008); L. Tiemann, Y. Yoon, W. Dietsche, K. von Klitzing, and W. Wegscheider, Phys. Rev. B **80**, 165120 (2009); Y. Yoon, L. Tiemann, S. Schmult, W. Dietsche, K. von Klitzing, and W. Wegscheider Phys. Rev. Lett. **104**, 116802 (2010).

[12] Z. F. Ezawa, S. Suzuki and G. Tsitsishvili, Phys. Rev. B **76**, 045307 (2007).

[13] Z. F. Ezawa, G. Tsitsishvili, and A. Sawada, Eur. Phys. J. B (2012) **85**: 270.

[14] L. Zheng, R. J. Radtke, and S. Das Sarma, Phys. Rev. Lett. **78**, 2453 (1997); S. Das Sarma, S. Sachdev, and L. Zheng, Phys. Rev. Lett. **79**, 917 (1997); Phys. Rev. B **58**, 4672 (1998).

[15] V. Pellegrini, A. Pinczuk, B. S. Dennis, A. S. Plaut, L. N. Pfeiffer, and K. W. West, Phys. Rev. Lett. **78**, 310 (1997); V. Pellegrini, A. Pinczuk, B. S. Dennis, A. S. Plaut, L. N. Pfeiffer, and K. W. West, Science **281**, 779 (1998).

[16] V. S. Khrapai, E. V. Deviatov, A. A. Shashkin, V. T. Dolgopolov, F. Hastreiter, A. Wixforth, K. L. Campman, and A. C. Gossard, Phys. Rev. Lett. **84**, 725 (2000).

[17] A. Fukuda, A. Sawada, S. Kozumi, D. Terasawa, Y. Shimoda, and Z. F. Ezawa, N. Kumada, and Y. Hirayama, Phys. Rev. B **73**, 165304 (2006).

[18] K. Hasebe and Z.F. Ezawa, Phys. Rev. B **66**, 155318 (2002).

[19] Y. Hama, Y. Hidaka, G. Tsitsishvili, and Z. F. Ezawa, Eur. Phys. J. B (2012) **85**: 368.

[20] Y. Hama, George. Tsitsishvili, and Zyun. F. Ezawa, Phys. Rev. B **87**, 104516 (2013).

[21] Z. F. Ezawa and G. Tsitsishvili, Phys. Rev. B **70**, 125304 (2004).

[22] Z. F. Ezawa, M. Eliashvili and G. Tsitsishvili, Phys. Rev. B **71**, 125318 (2005).

[23] M. Gell-Mann and Y. Ne'eman, *The eight-fold Way*, (Benjamin, New York, 1964).

Appendix A: Appendix A SU(4) algebra

The special unitary group SU(N) has $(N^2 - 1)$ generators. According to the standard notation from elementary particle physics[23], we denote them as λ_A, $A = 1, 2, \ldots, N^2 - 1$, which are represented by Hermitian, traceless, $N \times N$ matrices, and normalize them as

$$\mathrm{Tr}(\lambda_A \lambda_B) = 2\delta_{AB}. \tag{A1}$$

They are characterized by

$$[\lambda_A, \lambda_B] = 2if_{ABC}\lambda_C, \quad \{\lambda_A, \lambda_B\} = \frac{4}{N}2d_{ABC}\lambda_C, \tag{A2}$$

where f_{ABC} and d_{ABC} are the structure constants of SU(N). We have $\lambda_A = \tau_A$ (the Pauli matrix) with $f_{ABC} = \epsilon_{ABC}$ and $d_{ABC} = 0$ in the case of SU(2).

This standard representation is not convenient for our purpose because the spin group is SU(2) $\times$ SU(2) in the bilayer electron system with the four-component electron field as $\Psi = (\psi^{\mathrm{f\uparrow}}, \psi^{\mathrm{f\downarrow}}, \psi^{\mathrm{b\uparrow}}, \psi^{\mathrm{b\downarrow}})$. Embedding SU(2) $\times$ SU(2) into SU(4) we define the spin matrix by

$$\tau_a^{\mathrm{spin}} = \begin{pmatrix} \tau_a & 0 \\ 0 & \tau_a \end{pmatrix}, \tag{A3}$$

where $a = x, y, z$, and the pseudospin matrices by,

$$\tau_x^{\mathrm{ppin}} = \begin{pmatrix} 0 & \mathbf{1}_2 \\ \mathbf{1}_2 & 0 \end{pmatrix}, \quad \tau_y^{\mathrm{ppin}} = \begin{pmatrix} 0 & -i\mathbf{1}_2 \\ i\mathbf{1}_2 & 0 \end{pmatrix}, \quad \tau_z^{\mathrm{ppin}} = \begin{pmatrix} \mathbf{1}_2 & 0 \\ 0 & -\mathbf{1}_2 \end{pmatrix}, \tag{A4}$$

where $\mathbf{1}_2$ is the unit matrix in two dimensions. Nine remaining matrices are simple products of the spin and pseudospin matrices:

$$\tau_a^{\mathrm{spin}}\tau_x^{\mathrm{ppin}} = \begin{pmatrix} 0 & \tau_a \\ \tau_a & 0 \end{pmatrix}, \quad \tau_a^{\mathrm{spin}}\tau_y^{\mathrm{ppin}} = \begin{pmatrix} 0 & -i\tau_a \\ i\tau_a & 0 \end{pmatrix}, \quad \tau_a^{\mathrm{spin}}\tau_z^{\mathrm{ppin}} = \begin{pmatrix} \tau_a & 0 \\ 0 & -\tau_a \end{pmatrix}. \tag{A5}$$

We denote them $T_{a0} \equiv \frac{1}{2}\tau_a^{\text{spin}}$, $T_{0a} \equiv \frac{1}{2}\tau_a^{\text{ppin}}$, $T_{ab} \equiv \frac{1}{2}\tau_a^{\text{spin}}\tau_b^{\text{ppin}}$. They satisfy the normalization condition

$$\text{Tr}(T_{\mu\nu}T_{\gamma\delta}) = \delta_{\mu\gamma}\delta_{\nu\delta}, \tag{A6}$$

and the commutation relations

$$[T_{\mu\nu}, T_{\gamma\delta}] = if_{\mu\nu,\gamma\delta,\mu'\nu'}T_{\mu'\nu'}, \tag{A7}$$

where $f_{\mu\nu,\gamma\delta,\mu'\nu'}$ is the SU(4) structure constant in the basis (A3)-(A5). Greek indices run over $0, x, y, z$.

From (74), (75), and (77), the explicit form of the isospin densities in terms of η_i is given by:

$$
\begin{aligned}
\mathcal{I}_{0x} =& -\cos\theta_\alpha \sin\theta_\beta \mathcal{I}_{0x}^{\text{c}} + \cos\theta_\alpha \cos\theta_\beta \cos\theta_\delta \mathcal{I}_{0z}^{\text{c}} - \sin\theta_\alpha \cos\theta_\beta \cos\theta_\delta \mathcal{I}_{xx}^{\text{c}} - \sin\theta_\alpha \sin\theta_\beta \mathcal{I}_{xz}^{\text{c}} \\
& - \cos\theta_\alpha \cos\theta_\beta \sin\theta_\delta \mathcal{I}_{yy}^{\text{c}} + \sin\theta_\alpha \cos\theta_\beta \sin\theta_\delta \mathcal{I}_{z0}^{\text{c}}, \\
\mathcal{I}_{0y} =& \cos\theta_\delta \mathcal{I}_{0y}^{\text{c}} + \sin\theta_\delta \mathcal{I}_{yz}^{\text{c}}, \\
\mathcal{I}_{0z} =& -\cos\theta_\alpha \cos\theta_\beta \mathcal{I}_{0x}^{\text{c}} - \cos\theta_\alpha \sin\theta_\beta \cos\theta_\delta \mathcal{I}_{0z}^{\text{c}} + \sin\theta_\alpha \sin\theta_\beta \cos\theta_\delta \mathcal{I}_{xx}^{\text{c}} - \sin\theta_\alpha \cos\theta_\beta \mathcal{I}_{xz}^{\text{c}} \\
& + \cos\theta_\alpha \sin\theta_\beta \sin\theta_\delta \mathcal{I}_{yy}^{\text{c}} - \sin\theta_\alpha \sin\theta_\beta \sin\theta_\delta \mathcal{I}_{z0}^{\text{c}}, \\
\mathcal{I}_{x0} =& \cos\theta_\delta \mathcal{I}_{x0}^{\text{c}} - \sin\theta_\delta \mathcal{I}_{zx}^{\text{c}}, \\
\mathcal{I}_{xx} =& -\sin\theta_\alpha \cos\theta_\beta \mathcal{I}_{0x}^{\text{c}} - \sin\theta_\alpha \sin\theta_\beta \cos\theta_\delta \mathcal{I}_{0z}^{\text{c}} - \cos\theta_\alpha \sin\theta_\beta \cos\theta_\delta \mathcal{I}_{xx}^{\text{c}} + \cos\theta_\alpha \cos\theta_\beta \mathcal{I}_{xz}^{\text{c}} \\
& + \sin\theta_\alpha \sin\theta_\beta \sin\theta_\delta \mathcal{I}_{yy}^{\text{c}} + \cos\theta_\alpha \sin\theta_\beta \sin\theta_\delta \mathcal{I}_{z0}^{\text{c}}, \\
\mathcal{I}_{xy} =& \mathcal{I}_{xy}^{\text{c}}, \\
\mathcal{I}_{xz} =& \sin\theta_\alpha \sin\theta_\beta \mathcal{I}_{0x}^{\text{c}} - \sin\theta_\alpha \cos\theta_\beta \cos\theta_\delta \mathcal{I}_{0z}^{\text{c}} - \cos\theta_\alpha \cos\theta_\beta \cos\theta_\delta \mathcal{I}_{xx}^{\text{c}} - \cos\theta_\alpha \sin\theta_\beta \mathcal{I}_{xz}^{\text{c}} \\
& + \sin\theta_\alpha \cos\theta_\beta \sin\theta_\delta \mathcal{I}_{yy}^{\text{c}} + \cos\theta_\alpha \cos\theta_\beta \sin\theta_\delta \mathcal{I}_{z0}^{\text{c}}, \\
\mathcal{I}_{y0} =& \cos\theta_\alpha \mathcal{I}_{y0}^{\text{c}} - \sin\theta_\alpha \mathcal{I}_{zy}^{\text{c}}, \\
\mathcal{I}_{yx} =& -\cos\theta_\beta \sin\theta_\delta \mathcal{I}_{0y}^{\text{c}} - \sin\theta_\beta \mathcal{I}_{yx}^{\text{c}} + \cos\theta_\beta \cos\theta_\delta \mathcal{I}_{yz}^{\text{c}}, \\
\mathcal{I}_{yy} =& \cos\theta_\alpha \sin\theta_\delta \mathcal{I}_{0z}^{\text{c}} - \sin\theta_\alpha \sin\theta_\delta \mathcal{I}_{xx}^{\text{c}} + \cos\theta_\alpha \cos\theta_\delta \mathcal{I}_{yy}^{\text{c}} - \sin\theta_\alpha \cos\theta_\delta \mathcal{I}_{z0}^{\text{c}}, \\
\mathcal{I}_{yz} =& \sin\theta_\beta \sin\theta_\delta \mathcal{I}_{0y}^{\text{c}} - \cos\theta_\beta \mathcal{I}_{yx}^{\text{c}} - \sin\theta_\beta \cos\theta_\delta \mathcal{I}_{yz}^{\text{c}}, \\
\mathcal{I}_{z0} =& \sin\theta_\alpha \sin\theta_\delta \mathcal{I}_{0z}^{\text{c}} + \cos\theta_\alpha \sin\theta_\delta \mathcal{I}_{xx}^{\text{c}} + \sin\theta_\alpha \cos\theta_\delta \mathcal{I}_{yy}^{\text{c}} + \cos\theta_\alpha \cos\theta_\delta \mathcal{I}_{z0}^{\text{c}}, \\
\mathcal{I}_{zx} =& -\sin\theta_\beta \sin\theta_\delta \mathcal{I}_{x0}^{\text{c}} - \sin\theta_\beta \cos\theta_\delta \mathcal{I}_{zx}^{\text{c}} + \cos\theta_\beta \mathcal{I}_{zz}^{\text{c}}, \\
\mathcal{I}_{zy} =& \sin\theta_\alpha \mathcal{I}_{y0}^{\text{c}} + \cos\theta_\alpha \mathcal{I}_{zy}^{\text{c}}, \\
\mathcal{I}_{zz} =& -\cos\theta_\beta \sin\theta_\delta \mathcal{I}_{x0}^{\text{c}} - \cos\theta_\beta \cos\theta_\delta \mathcal{I}_{zx}^{\text{c}} - \sin\theta_\beta \mathcal{I}_{zz}^{\text{c}}.
\end{aligned} \tag{A8}
$$

where we defined $\mathcal{I}_{a0} \equiv \mathcal{S}_a, \mathcal{I}_{0a} \equiv \mathcal{P}_a, \mathcal{I}_{ab} \equiv \mathcal{R}_{ab}$ and

$$\mathcal{I}_{0x}^{\mathrm{c}} = \mathrm{Re}\left[\eta_1^\dagger \eta_3 + \eta_4^\dagger \eta_2 - \eta_4^\dagger \eta_1 - \eta_2^\dagger \eta_3\right], \quad \mathcal{I}_{0y}^{\mathrm{c}} = \mathrm{Im}\left[\eta_1^\dagger \eta_3 + \eta_4^\dagger \eta_2 - \eta_4^\dagger \eta_1 - \eta_2^\dagger \eta_3\right],$$

$$\mathcal{I}_{0z}^{\mathrm{c}} = |\eta_4|^2 - |\eta_3|^2,$$

$$\mathcal{I}_{x0}^{\mathrm{c}} = \mathrm{Re}[\eta_1 + \eta_2], \quad \mathcal{I}_{xx}^{\mathrm{c}} = \mathrm{Re}[\eta_3 + \eta_4], \quad \mathcal{I}_{xy}^{\mathrm{c}} = \mathrm{Im}[\eta_3 - \eta_4], \quad \mathcal{I}_{xz}^{\mathrm{c}} = \mathrm{Re}[\eta_1 - \eta_2],$$

$$\mathcal{I}_{y0}^{\mathrm{c}} = \mathrm{Im}[\eta_1 + \eta_2], \quad \mathcal{I}_{yx}^{\mathrm{c}} = \mathrm{Im}[\eta_3 + \eta_4], \quad \mathcal{I}_{yy}^{\mathrm{c}} = -\mathrm{Re}[\eta_3 - \eta_4], \quad \mathcal{I}_{yz}^{\mathrm{c}} = \mathrm{Im}[\eta_1 - \eta_2],$$

$$\mathcal{I}_{z0}^{\mathrm{c}} = 1 - \sum_{i=1}^{4} |\eta_i|^2, \quad \mathcal{I}_{zx}^{\mathrm{c}} = -\mathrm{Re}\left[\eta_1^\dagger \eta_3 + \eta_4^\dagger \eta_2 + \eta_4^\dagger \eta_1 + \eta_2^\dagger \eta_3\right],$$

$$\mathcal{I}_{zy}^{\mathrm{c}} = -\mathrm{Im}\left[\eta_1^\dagger \eta_3 + \eta_4^\dagger \eta_2 + \eta_4^\dagger \eta_1 + \eta_2^\dagger \eta_3\right], \quad \mathcal{I}_{zz}^{\mathrm{c}} = |\eta_2|^2 - |\eta_1|^2. \tag{A9}$$

From (A8), (A9), and the equal-time commutation relations (79), it can be verified that the SU(4) algebraic relation

$$[\mathcal{I}_{\mu\nu}(\boldsymbol{x}, t), \mathcal{I}_{\gamma\delta}(\boldsymbol{x}, t)] = i\delta(\boldsymbol{x} - \boldsymbol{y}) f_{\mu\nu,\gamma\delta,\mu'\nu'} \mathcal{I}_{\mu'\nu'}(\boldsymbol{y}, t), \tag{A10}$$

is held.